Title

Mammalian Protein Arginine Methyltransferase 7 (PRMT7) Specifically Targets RXR Sites in Lysine- and Arginine-rich Regions*

Journal

Journal of Biological Chemistry, 288(52)

ISSN

0021-9258

Authors

Feng, You
Maity, Ranjan
Whitelegge, Julian P
et al.

Publication Date

2013-12-01

DOI

10.1074/jbc.m113.525345

Peer reviewed

THE JOURNAL OF BIOLOGICAL CHEMISTRY VOL. 288, NO. 52, pp. 37010–37025, December 27, 2013

Mammalian Protein Arginine Methyltransferase 7 (PRMT7) Specifically Targets R*X*R Sites in Lysine- and Arginine-rich Regions*

Received for publication, October 7, 2013, and in revised form, November 1, 2013 Published, JBC Papers in Press, November 18, 2013, DOI 10.1074/jbc.M113.525345

You Feng[‡], Ranjan Maity[§], Julian P. Whitelegge[¶], Andrea Hadjikyriacou[‡], Ziwei Li[‖], Cecilia Zurita-Lopez[‡], Qais Al-Hadid[‡], Amander T. Clark[‖], Mark T. Bedford[**], Jean-Yves Masson[§], and Steven G. Clarke[‡1]

*From the Departments of [‡]Chemistry and Biochemistry and [‖]Molecular, Cellular, and Developmental Biology, Molecular Biology Institute, UCLA, Los Angeles, California 90095, the [§]Genome Stability Laboratory, Laval University Cancer Research Center, Hôtel-Dieu de Québec Research Center, Québec G1R 2J6, Canada, the [¶]Pasarow Mass Spectrometry Laboratory, NPI-Semel Institute for Neuroscience and Human Behavior UCLA, Los Angeles, California 90095, and the **Department of Molecular Carcinogenesis, University of Texas MD Anderson Cancer Center, Smithville, Texas 78957*

Background: Protein arginine methyltransferase 7 (PRMT7) is associated with various functions and diseases, but its substrate specificity is poorly defined.
Results: Insect cell-expressed PRMT7 forms ω-monomethylarginine residues at basic R*X*R sequences in peptides and histone H2B.
Conclusion: PRMT7 is a type III PRMT with a unique substrate specificity.
Significance: Novel post-translational modification sites generated by PRMT7 may regulate biological function.

The mammalian protein arginine methyltransferase 7 (PRMT7) has been implicated in roles of transcriptional regulation, DNA damage repair, RNA splicing, cell differentiation, and metastasis. However, the type of reaction that it catalyzes and its substrate specificity remain controversial. In this study, we purified a recombinant mouse PRMT7 expressed in insect cells that demonstrates a robust methyltransferase activity. Using a variety of substrates, we demonstrate that the enzyme only catalyzes the formation of ω-monomethylarginine residues, and we confirm its activity as the prototype type III protein arginine methyltransferase. This enzyme is active on all recombinant human core histones, but histone H2B is a highly preferred substrate. Analysis of the specific methylation sites within intact histone H2B and within H2B and H4 peptides revealed novel post-translational modification sites and a unique specificity of PRMT7 for methylating arginine residues in lysine- and arginine-rich regions. We demonstrate that a prominent substrate recognition motif consists of a pair of arginine residues separated by one residue (R*X*R motif). These findings will significantly accelerate substrate profile analysis, biological function study, and inhibitor discovery for PRMT7.

Post-translational modifications dramatically increase the diversity of proteins in the cell and substantially contribute to epigenetic regulation and the control of cellular processes (1). One of the major groups of enzymes that catalyze these reactions in eukaryotic cells are protein arginine methyltransferases (PRMTs)[2] that transfer methyl groups from the methyl donor, *S*-adenosyl-*L*-methionine (AdoMet), to specific arginine residues on protein substrates (Fig. 1). In mammals, a group of nine sequence-related PRMTs have been characterized (2, 3). PRMT1, -2, -3, -4, -6, and -8 catalyze the formation of ω-N^G-monomethylarginine (MMA) and ω-N^G, N^G-asymmetric dimethylarginine (ADMA) and are classified as type I PRMTs. PRMT5 catalyzes the formation of MMA and ω-N^G, N'^G-symmetric dimethylarginine (SDMA) and is defined as a type II PRMT. More recently, PRMT7 has emerged as a type III PRMT that produces only MMA in its substrates (4, 5). In humans and mice, PRMT7 is a 692-amino acid protein with an ancestral duplication of the catalytic domains, both of which are required for its activity (4). PRMT7, when expressed as a GFP fusion protein, shows a predominantly cytoplasmic distribution (6).

The physiological roles of PRMT7 have been associated with broad cellular processes in mammalian cells (3, 7). It has been indicated that PRMT7 may play a role in Sm protein methylation and small nuclear ribonucleoprotein biogenesis (8). PRMT7 knockdown up-regulates the expression of genes involved in DNA repair, including ALKBH5, APEX2, POLD1, and POLD2 (9). It has also been suggested that PRMT7 plays a role in pluripotency state maintenance in undifferentiated embryonic stem cells and germ cells (10) and antagonizes MLL4-mediated differentiation (11). Interestingly, PRMT7 has been associated with cellular sensitivity to a number of drugs.

* This work was supported, in whole or in part, by National Institutes of Health Grants GM026020 (to S. G. C.), S10 RR023045 (to J. P. W.), and DK62248 (to M. T. B.). This work was also supported by the Canadian Institute of Health Research (to J. Y. M.).
[1] To whom correspondence should be addressed: Dept. of Chemistry and Biochemistry and the Molecular Biology Institute, UCLA, 607 Charles E. Young Dr. East, Los Angeles, CA. Tel.: 310-825-8754; Fax: 310-825-1968; E-mail: clarke@chem.ucla.edu.

[2] The abbreviations used are: PRMT, protein arginine methyltransferase; MMA, ω-N^G-monomethylarginine; ADMA, ω-N^G, N^G-asymmetric dimethylarginine; SDMA, ω-N^G,N'^G-symmetric dimethylarginine; AdoMet, *S*-adenosyl-L-methionine; [^{3}H]AdoMet, *S*-adenosyl-[*methyl*-^{3}H]L-methionine; HBR, H2B repression region; BisTris, 2-[bis(2-hydroxyethyl)amino]-2-(hydroxymethyl)propane-1,3-diol; ESI, electrospray ionization; ETD, electron transfer dissociation.

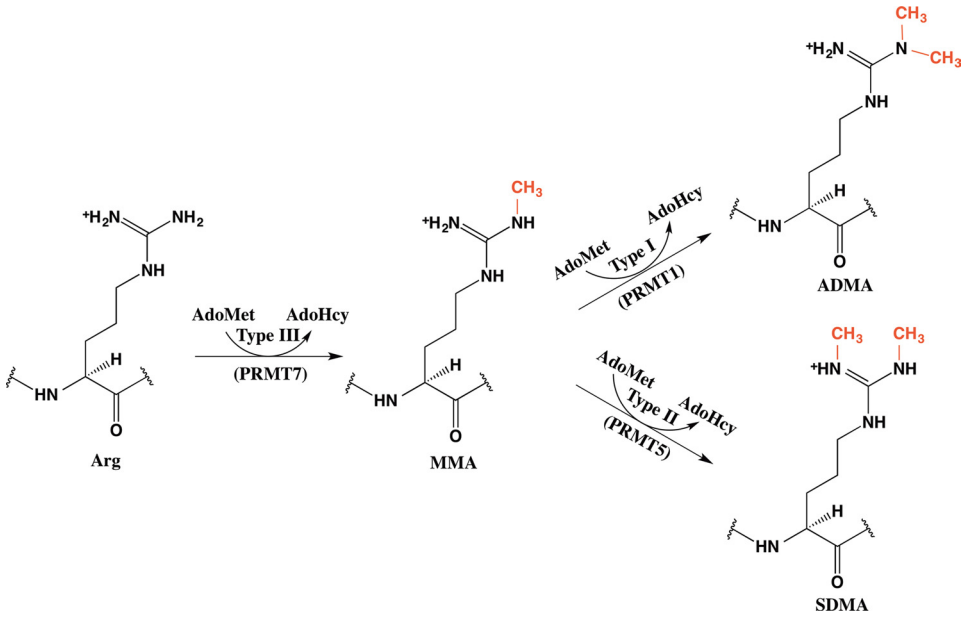

FIGURE 1. **Reactions catalyzed by type I, II, and III PRMTs.** AdoHcy, *S*-adenosylhomocysteine.

Its expression has been correlated with sensitivity to topoisomerase II inhibitors in Chinese hamster fibroblasts (12), resistance to the topoisomerase I inhibitor camptothecin in HeLa cells (13), and correlated by linkage-directed association analysis to etoposide cytotoxicity in human lymphoblastoid cell lines (14). Finally, a gene expression meta-analysis identified a possible role of PRMT7 in promoting breast cancer metastasis (15). These results suggest PRMT7 as a potential target for anticancer therapeutics.

Since its discovery as a methyltransferase (4), the type of methylation reaction catalyzed by PRMT7 has been under debate. A sole type III activity forming MMA has been reported (4, 5) as well as a type I/type II activity forming both ADMA and SDMA (16). A sole type III activity was also found for the worm and trypanosome homologs of PRMT7 (17, 18). In a number of studies, PRMT7 was expressed in mammalian cells as a FLAG-tagged species where the purification methods would be expected to also pull down the type II PRMT5 species (2, 3, 19). The potential contamination of PRMT7 with PRMT5 (and possibly other PRMTs, including the major PRMT1 species) in such studies would complicate the analysis of substrate specificity. These problems may have led to the misclassification of PRMT7 as a type II PRMT and confusion of its methylation sites with those of other PRMTs (9, 20). Given the roles of PRMTs in epigenetic regulation via histone methylation and the involvement of PRMT7 in both cell development and cancer (10–15), it is important to establish the catalytic pattern and substrate specificity of PRMT7.

Here, we report the expression and purification of mouse PRMT7 from insect cells with robust activity. We identify H2B as the best substrate among recombinant human core histones and detect the monomethylation of H2B Arg-29, Arg-31, Arg-33 and H4 Arg-17, Arg-19 by PRMT7 with high resolution amino acid analysis and top-down mass spectroscopy. We found that PRMT7 specifically targets arginine residues in R*X*R motifs surrounded by multiple lysines. Our work confirming the type III formation of MMA and our discovery of the unique substrate recognition motif of PRMT7 clarify two common ambiguities in the study of this methyltransferase, setting a foundation for exploring the kinetic mechanism, inhibitor discovery, and biological functions of PRMT7.

EXPERIMENTAL PROCEDURES

Mutagenesis—Mouse PRMT7-pEGFP-C1 plasmid was prepared as described (6). The wild-type plasmid was mutated to create a catalytically inactive enzyme that cannot bind AdoMet, with motif I residues LDIG changed to AAAA. Mutagenic primers were designed to be 45 bases in length with a T_m of 89 °C. Primers used were as follows: forward primer 5′-GGA CAG AAG GCC TTG GTT GCG GCC GCT GCG ACT GGC ACG GGA CTC-3′ and reverse primer 5′-GAG TCC CGT GCC AGT CGC AGC GGC CGC AAC CAA GGC CTT CTG TCC-3′. A PCR was set up according to the QuikChange site-directed mutagenesis kit (Agilent), using 50 ng of dsDNA template (GFP-PRMT7 wild type), 125 ng of both primers, and PfuUltra HF DNA polymerase. The PCR was run at 95 °C for 1 min, 18 cycles of 95 °C for 50 s, 60 °C for 50 s, and 68 °C for 10 min. There was an additional 7-min extension at 68 °C. Amplification products were then digested using 10 units of DpnI for 1 h at 37 °C to remove the parental dsDNA. Plasmids were then transformed into XL10-Gold ultracompetent *Escherichia coli* cells, plated on LB kanamycin plates, and grown overnight at 37 °C. Positive colonies were subjected to DNA sequencing on both strands to confirm the mutations (GeneWiz, Inc.).

Protein Expression and Purification—Wild-type and mutant mouse GFP-PRMT7 plasmid DNA prepared as described above were subcloned into a modified pFastBac baculovirus expression vector and expressed between GST (at the N terminus) and His tag (at the C terminus). The PRMT7 pFastBac vector was transformed into *E. coli* (DH10Bac), and the bacmid DNA was generated. *Spodoptera frugiperda* (Sf9) insect cells were then transfected with the bacmid DNA to produce virus particles. By

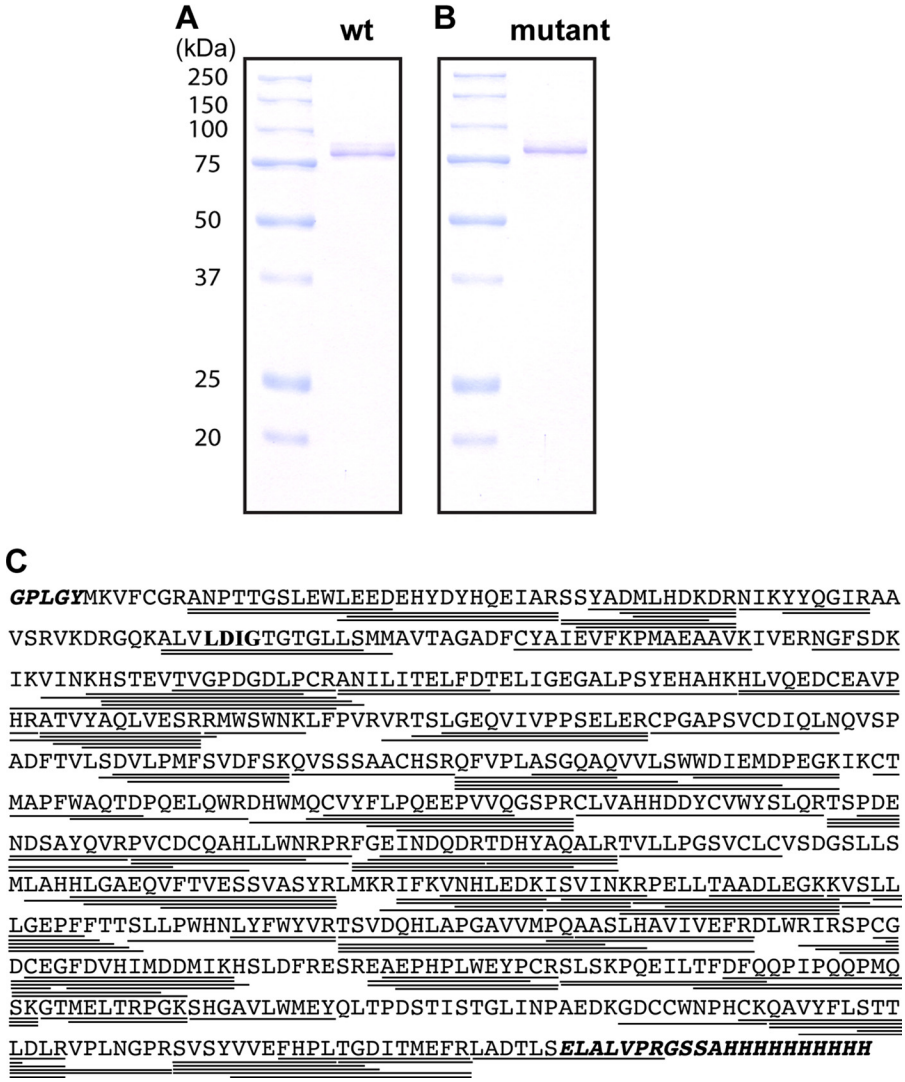

FIGURE 2. **Recombinant mouse PRMT7 expressed in Sf9 insect cells.** *A,* SDS-PAGE followed by Coomassie Blue staining of the purified wild-type enzyme, revealing a single major polypeptide of ~80 kDa (expected mass is 81.2 kDa). This protein includes an N-terminal extension of GPLGY and a C-terminal extension of ELALVPRGSSAHHHHHHHHHH. The lane of marker proteins is shown on the *left* with the polypeptide sizes. *B,* SDS-PAGE analysis of the PRMT7 inactive mutant with motif I residues LDIG changed to AAAA. *C,* LC-MS/MS analysis of tryptic peptides of wild-type PRMT7. Sequences were searched against both the *S. frugiperda* and the mouse subsets of the UniRef100 database as well as the tagged expected sequence of PRMT7. Sequence coverage of the recombinant PRMT7 (85%) is shown by *underlining*; those residues not present in the endogenous protein are highlighted in *bold* and *italics*; the LDIG motif that was mutated in the PRMT7 mutant is shown in *bold*.

performing mini-infection assays, we selected the most efficient conditions for protein expression, which were 0.75–1.0 × 10^6 cells/ml with a ratio of 1:100 between virus suspension and media and 48 h of duration for infection. One liter of Sf9 cell culture pellet (infected with wild-type or mutant PRMT7-expressing baculovirus) was used for protein purification. The Sf9 cell pellet was lysed in 40 ml of PBS lysis buffer containing 1 mM EDTA, 0.05% Triton X-100, 1 mM DTT, 1 tablet of protease inhibitor mixture (Roche Applied Science), and a final concentration of 250 mM NaCl, using 20 strokes of a Dounce homogenizer followed by three 30-s periods of sonication. The total cell lysate was incubated for 30 min at 4 °C with 1 mM $MgCl_2$ and benzonase nuclease to remove DNA or RNA contamination followed by centrifugation at 38,724 × *g* for 30 min at 4 °C to get a clear soluble lysate. The soluble cell lysate was then incubated with Glutathione-Sepharose 4B beads (GE Healthcare) for 1 h in GST-binding buffer (lysis buffer without protease inhibitor) followed by washing the beads three times with washing buffer (GST binding buffer made up to a final concentration of 350 mM NaCl). The GST beads were then incubated with 5 mM ATP and 15 mM $MgCl_2$ for 1 h at 4 °C to prevent nonspecific binding of heat-shock proteins and washed again three times with washing buffer. GST beads were then washed with P5 buffer (50 mM sodium phosphate, 500 mM NaCl, 10% glycerol, 0.05% Triton X-100, 5 mM imidazole, pH 7.0) and incubated with PreScission protease (GE Healthcare; 4–8 units for 100 μl of GST beads) in P5 buffer for 6 h at 4 °C. GST-cleaved PRMT7 protein was collected as the supernatant after centrifugation and incubated with TALON cobalt metal affinity resin (Clontech; prewashed with P5 buffer) for 1 h in P5 buffer at 4 °C under rotation. The TALON resin was then washed three times (5 min each) with P30 buffer (P5 buffer with a final concentration of 30 mM imidazole). PRMT7 protein was then eluted from the resin with P500 buffer (P5 buffer with a final

concentration of 500 mM imidazole) with 5 min under rotation, and the elution step was repeated two times to elute maximum protein (21). Purified PRMT7 protein was analyzed for quality and quantity by SDS-PAGE with Coomassie Blue staining. The final sequence is GPLGY-(mouse PRMT7)-ELALVPRGSSAH-HHHHHHHHH, as shown in Fig. 2. PRMT7 protein was then dialyzed in storage buffer (Tris-Cl, pH 7.5, 150 mM NaCl, 10% glycerol, 1 mM DTT) at 4 °C for 1 h and stored in small aliquots at −80 °C.

PRMT1 was used as a His-tagged species purified from *E. coli* (22, 23) and was a kind gift from Drs. Heather Rust and Paul Thompson (Scripps Research Institute, Jupiter, FL). PRMT5 was used as a Myc-tagged species purified from HEK293 cells (24) and was a kind gift from Drs. Jill Butler and Sharon Dent (University of Texas MD Anderson Cancer Center, Houston, TX).

Peptide and Protein Substrates—Peptides H2B(23-37), H2B(23-37)R29K, H2B(23-37)R31K, H2B(23-37)R33K, H2B(23-37)R29K,R31K, H2B(23-37)R29K,R33K, H2B(23-37)R31K,R33K, H4(1-8), H4(14-22), H4(14-22)R17K, and H4(14-22)R19K were purchased from GenScript as HPLC-purified materials at >90% purity and verified by mass spectrometry by the vendor. Peptides H4(1-21), H4(1-21)R3K and H4(1-21)R3MMA were previously described (22, 23) and were a kind gift of Drs. Heather Rust and Paul Thompson (Scripps Research Institute). The sequences of all the peptides are listed in Table 1. GST-GAR was expressed in *E. coli* BL21 Star (DE3) cells (Invitrogen, C601003) and purified with glutathione-Sepharose 4B beads (Amersham Biosciences) by affinity chromatography as described previously (5). Recombinant human histone H2A (GenBank™ accession number AAN59960), H2B (GenBank™ accession number AAN59961), H3.3 (GenBank™ accession number P84243), and H4 (GenBank™ accession number AAM83108) were purchased from New England Biolabs as 1 mg/ml solutions in 20 mM sodium phosphate, 300 mM NaCl, and 1 mM EDTA. Histone H3.3 also included 1 mM DTT. In some cases, the histone preparations were dialyzed against 10,000 volumes of the reaction buffer (50 mM potassium HEPES, 10 mM NaCl and 1 mM DTT, pH 7.5) or H_2O, at 4 °C for 1 h. Alternatively, the original buffer was exchanged by diluting histones 40-fold in the reaction buffer and then reconcentrated using an Amicon centrifugation filter; this process was repeated twice.

In Vitro Methylation Assay and Acid Hydrolysis of Protein and Peptide Substrates—PRMT-catalyzed reactions were performed with 0.7 μM *S*-adenosyl-L-[*methyl*-^{3}H]methionine ([^{3}H]AdoMet; PerkinElmer Life Sciences, 75–85 Ci/mmol, from a stock of 0.55 mCi/ml in 10 mM H_2SO_4/EtOH (9:1, v/v)) and appropriate substrate in a final reaction volume of 60 μl unless otherwise specified. The reactions were buffered in 50 mM potassium HEPES, pH 7.5, 10 mM NaCl, and 1 mM DTT and incubated at room temperature (21–23 °C) for 20–24 h. When proteins were used as substrates, the methylation reactions were quenched with 12.5% (w/v) trichloroacetic acid, and 20 μg of bovine serum albumin was added as a carrier protein. After incubation at room temperature for 30 min, the precipitated protein was collected by centrifugation at 4000 × *g* for 30 min. The pellet was washed with cold acetone and air-dried. When peptides were used as substrates, the reaction mixture was quenched with trichloroacetic acid (final concentration is 1.6%), and peptides were isolated using an OMIX C18 ZipTip (Agilent Technologies) followed by vacuum centrifugation. Acid hydrolysis of all dried reaction mixtures was then carried out *in vacuo* at 110 °C for 20 h using 50 μl of 6 N HCl. Samples were then dried by vacuum centrifugation and dissolved in 50 μl of water.

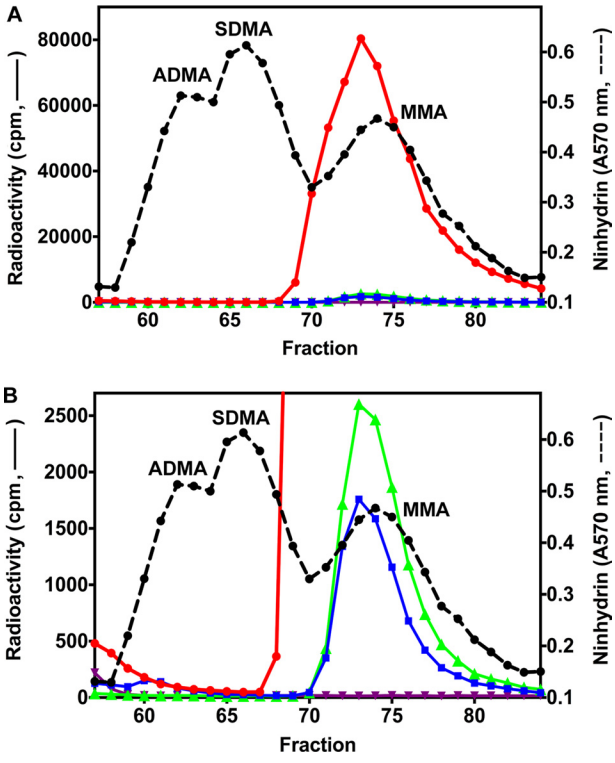

FIGURE 3. **Formation of [^{3}H]MMA from incubation of PRMT7 with [^{3}H]AdoMet and GST-GAR as a methyl-accepting substrate.** *A, in vitro* methylation reactions were performed as described under "Experimental Procedures" using 6 μg of GST-GAR and 1.2 μg of wild-type or mutant PRMT7 at a final concentration of 0.26 μM. Incubations in the absence of PRMT7 or GST-GAR were used as controls. The reactions were allowed to proceed at room temperature for 20 h. After acid hydrolysis, the methylated amino acid derivatives were analyzed by high resolution cation exchange chromatography together with standards of ADMA, SDMA, and MMA as described under "Experimental Procedures." ^{3}H radioactivity (*solid lines*) and the ninhydrin color of the methylated arginine standards (*dashed lines*; elution positions indicated) were determined with liquid scintillation counting and 570 nm absorbance, respectively. Because of a tritium isotope effect (5), the [^{3}H]methyl derivatives of ADMA, SDMA, and MMA elute on the high resolution cation exchange chromatography column 1–2 min earlier than the nonisotopically labeled standards. *Red,* wild-type PRMT7 with GST-GAR; *green,* wild-type PRMT7 alone; *blue,* mutant PRMT7 with GST-GAR; *purple,* GST-GAR alone. *B,* magnification of the radioactivity scale to show PRMT7 automethylation (*green*), the residual activity of mutant PRMT7 (*blue*), and the absence of ADMA and SDMA in the reaction products (*red*).

Amino Acid Analysis of Methylation Products by High Resolution Cation Exchange Chromatography—Amino acid analysis was performed to determine the products of enzymatic methylation reactions as described previously (5). Briefly, the hydrolyzed samples were mixed with 1 μmol each of ω-MMA (acetate salt, Sigma, M7033), SDMA (di(*p*-hydroxyazobenzene)-*p*′-sulfonate salt, Sigma, D0390), and ADMA (hydrochloride salt, Sigma, D4268) as internal standards. Samples were loaded onto a cation exchange column of PA-35 sulfo-

TABLE 1

Sequences of synthesized H2B and H4 peptides

Ac is acetyl.

Peptide	Sequence	Theoretical M_r	Observed M_r
H2B(23–37)	Ac-KKDGKKRKRSRKESY	1936.23	1935.60[a]
H2B(23–37)R29K	Ac-KKDGKKKRSRKESY	1908.22	1908.00[a]
H2B(23–37)R31K	Ac-KKDGKKRKKSRKESY	1908.22	1907.80[a]
H2B(23–37)R33K	Ac-KKDGKKRKRSKKESY	1908.22	1908.00[a]
H2B(23–37)R29K,R31K	Ac-KKDGKKKKKSRKESY	1880.21	1879.60[a]
H2B(23–37)R29K,R33K	Ac-KKDGKKKKRSKKESY	1880.21	1879.60[a]
H2B(23–37)R31K,R33K	Ac-KKDGKKRKKSKKESY	1880.21	1879.60[a]
H4(1–21)	Ac-SGRGKGGKGLGKGGAKRHRKV	2132	2133[b]
H4(1–21)R3K	Ac-SGKGKGGKGLGKGGAKRHRKV	2104	2105[b]
H4(1–21)R3MMA	Ac-SGR(me)GKGGKGLGKGGAKRHRKV	2146	2147[b]
H4(1–8)	Ac-SGRGKGGK	787.87	787.60[a]
H4(14–22)	Ac-GAKRHRKVL	1106.33	1106.25[a]
H4(14–22)R17K	Ac-GAKKHRKVL	1078.32	1078.20[a]
H4(14–22)R19K	Ac-GAKRHKKVL	1078.32	1078.20[a]

[a] Data were provided by GenScript Inc.
[b] Data are from Refs. 22, 23.

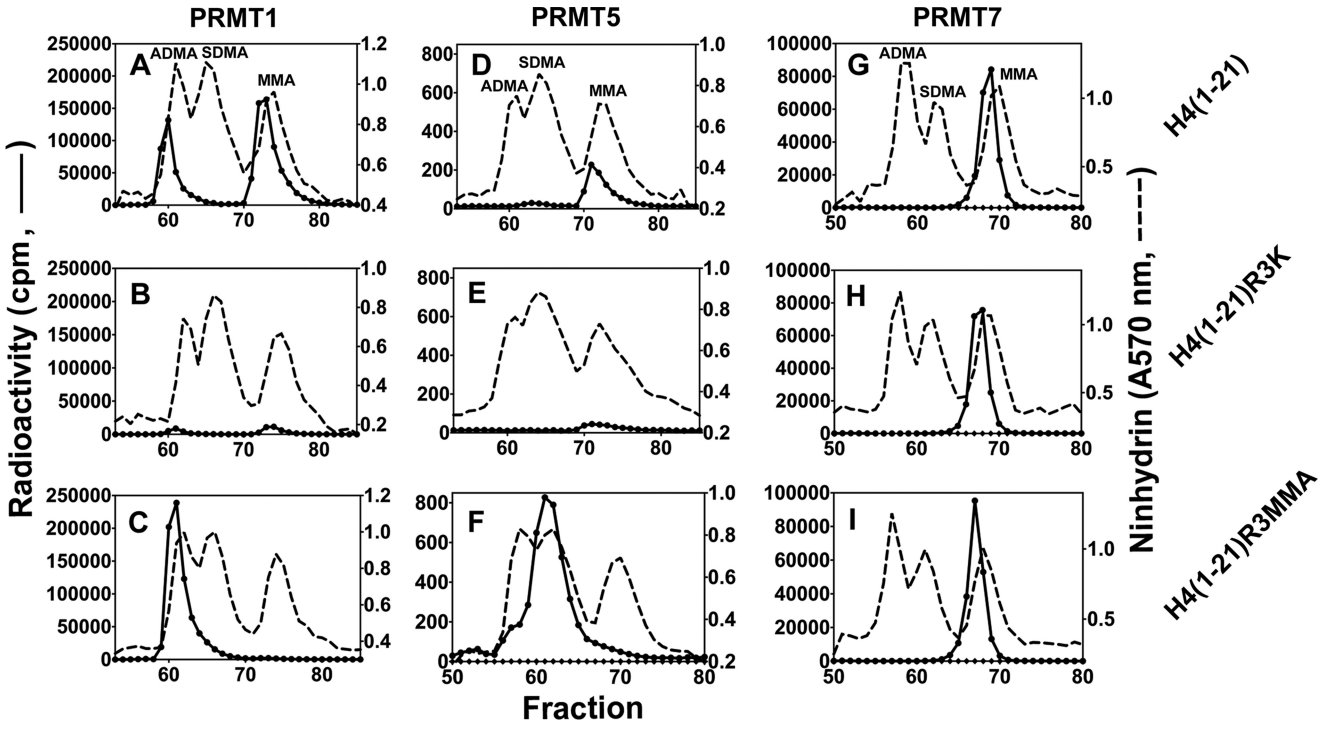

FIGURE 4. **Comparison of the methylation products of PRMT1, -5, and -7 using synthetic peptides derived from the N terminus of human histone H4.** Peptides (12.5 μM final concentration) were incubated with [^{3}H]AdoMet and PRMT1 (0.45 μM final concentration), PRMT5 (0.72 μM final concentration), or PRMT7 (0.26 μM final concentration) as described under "Experimental Procedures" and the reactions were allowed to proceed at room temperature for 20 h. The reaction mixtures were then acid-hydrolyzed and analyzed for methylated arginine species as described under "Experimental Procedures." *A–C* show PRMT1-catalyzed methylation products of peptides H4(1–21), H4(1–21)R3K, and H4(1–21)R3MMA (Table 1), respectively. *D–F* show PRMT5-catalyzed methylation products of these peptides. *G–I* show PRMT7-catalyzed methylation products of these peptides. The elution positions of the ADMA, SDMA, and MMA standards are specifically indicated in *A, D,* and *G* but are similar in all of the experiments.

nated polystyrene beads (6–12 μm; Benson Polymeric Inc., Sparks, NV) and eluted with sodium citrate buffer (0.35 M Na^+, pH 5.27) at 1 ml/min at 55 °C. Elution positions of the amino acid standards were determined by a ninhydrin assay. 50-μl aliquots of 1-ml column fractions were mixed with 100 μl of ninhydrin solution (20 mg/ml ninhydrin and 3 mg/ml hydrindantin in 75% (v/v) dimethyl sulfoxide and 25% (v/v) 4 M lithium acetate, pH 4.2) and incubated at 100 °C for 15–20 min, and the absorbance was measured at 570 nm using a SpectraMax M5 microplate reader with a path length of 0.5 cm. Radioactivity in column fractions was quantitated using a Beckman LS6500 counter and expressed as an average of three 5-min counting cycles after mixing 950 μl of each fraction with 10 ml of fluor (Safety Solve, Research Products International, 111177).

Fluorography of Histones Methylated by PRMT7—The enzymatic methylation reactions were set up with [^{3}H]AdoMet as described above. After 15–20 h of incubation at room temperature (21–23 °C), the reactions were quenched by SDS loading buffer and separated on 16% Tris-glycine gel (Novex, Invitrogen, EC6495BOX) or 4–12% BisTris gel (NuPAGE Novex, Invitrogen, NP0335BOX), stained with Coomassie Blue for 0.5 h, destained for 1 h, enhanced in autoradiography enhancing buffer (EN3HANCE™, PerkinElmer Life Sciences, 6NE9701) for 1 h, and vacuum-dried. The fluoroimage was

scanned after 3 h to 7 days of exposure to autoradiography film (Denville Scientific Inc., E3012). From the fluoroimage, the densitometry of each band was measured with ImageJ software, and the specific radioactivity was calculated by dividing the intensity of the fluorograph band with that of the Coomassie-stained band.

Top-down Mass Spectrometry of Proteins or Peptides Methylated by PRMT7—Methylation reactions were performed at the indicated concentration of AdoMet (Sigma, A2408, *p*-toluenesulfonate salt) in a buffer of 50 mM potassium HEPES, pH 7.5, 10 mM NaCl, and 1 mM DTT. Top-down mass spectrometry coupled with ETD (LTQ-Orbitrap) was used to determine the methylation sites targeted by PRMT7. Protein or peptide substrate was incubated with PRMT7 and 182–200 μM AdoMet in the reaction buffer at room temperature for 24 h. Then the methylation products were loaded onto OMIX C18 ZipTip (Agilent Technologies, A5700310), washed with 0.1% formic acid, and eluted with formic acid/acetonitrile/H_2O (0.1:50:50). The eluted sample was subjected directly to electrospray ionization (ESI), and ion isolation and ETD fragmentation were performed to identify and break down the positively charged methylated species. Unit resolution was achieved on all product ions by operating the instrument at 30,000 or 60,000 resolution (at 400 m/z). The mass spectra of multiply charged precursors were deconvoluted to monoisotopic zero-charge mass using Xtract 3.0 software. The ETD tandem mass spectra were analyzed with ProsightPC 2.0 software (Thermo Scientific) to match the identified c and z ions to the known amino acid sequences and to localize post-translational modifications, which remain a largely manual process.

RESULTS

Robust Mouse PRMT7 Expressed in Insect Cells Catalyzes the Formation of Monomethylated Arginine Residues Only—Previously, human PRMT7 was prepared as a GST fusion protein expressed in bacterial cells. This enzyme was shown to be a type III enzyme that formed MMA residues on a variety of proteins and peptides (4, 5). However, the enzymatic activity was relatively low. To study an enzyme with minimal exogenous residues that could be expressed in animal cells in potential complex with interacting proteins and with potential post-translational modifications, we prepared recombinant mouse PRMT7 with small N- and C-terminal tags in Sf9 insect cells. We observed a single major polypeptide of the expected size of PRMT7 with SDS-PAGE analysis (Fig. 2*A*). LC-MS/MS analysis demonstrated high sequence coverage (85%) of PRMT7 (Fig. 2*C*) and the absence of tryptic peptides corresponding to other PRMTs or other methyltransferases from mouse or *S. frugiperda*. Additionally, no tryptic peptides were detected consistent with the presence of additional stoichiometric subunits of PRMT7. As a control, a catalytic mutant was prepared where the AdoMet-binding motif I residues LDIG were changed to AAAA (Fig. 2*B*).

Methylation assays were then carried out with the previously characterized substrates GST-GAR, a protein containing the first 148 amino acids of human fibrillarin (5, 21), and synthetic peptides derived from the N terminus of human histone H4 (22, 23, 25–27). Using amino acid analysis employing high resolu-

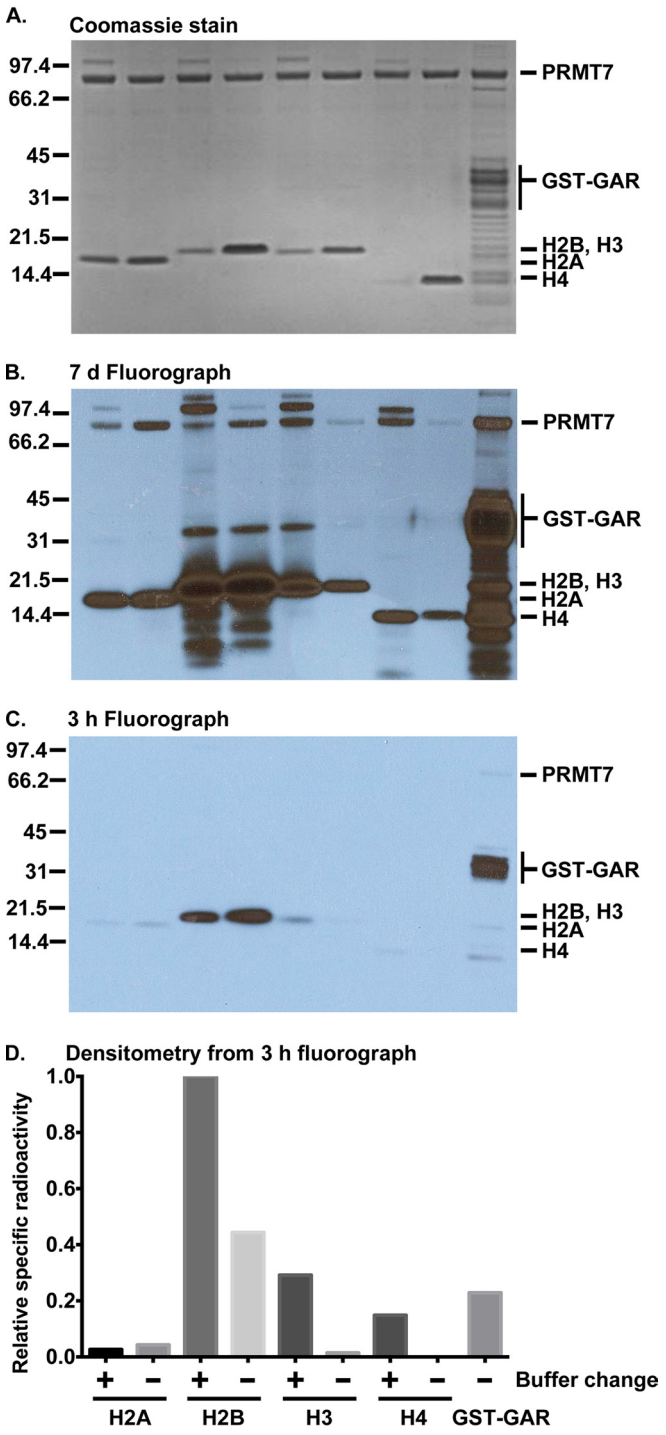

FIGURE 5. **PRMT7-catalyzed methylation of core histones with and without buffer change detected by fluorography.** 4 μg of human recombinant histones H2A, H2B, H3.3, and H4, either in the supplied buffer or exchanged into the reaction buffer (see "Experimental Procedures"), or 4 μg of GST-GAR were mixed with PRMT7 (0.26 μM final concentration) and [^{3}H]AdoMet and incubated at room temperature as described under "Experimental Procedures" for 20 h in a final volume of 40 μl. Samples were then mixed with SDS loading buffer, separated on 4–12% BisTris gel, and stained with Coomassie Blue (*A*). The protein substrate in each lane was labeled at the *bottom* of the graph. The expected position of molecular mass standards (Bio-Rad, broad range) is shown on the *left* in kDa. The fluoroimage was developed after 7 days (*d*) of film exposure (*B*) or 3 h of film exposure (*C*). As described under "Experimental Procedures," the density of radioactive bands from the film shown in *C* (where the density was mostly in the linear range) was divided by the density of the Coomassie-stained polypeptide to obtain the specific radioactivity (*D*). Data were normalized against the specific radioactivity of H2B (with buffer change).

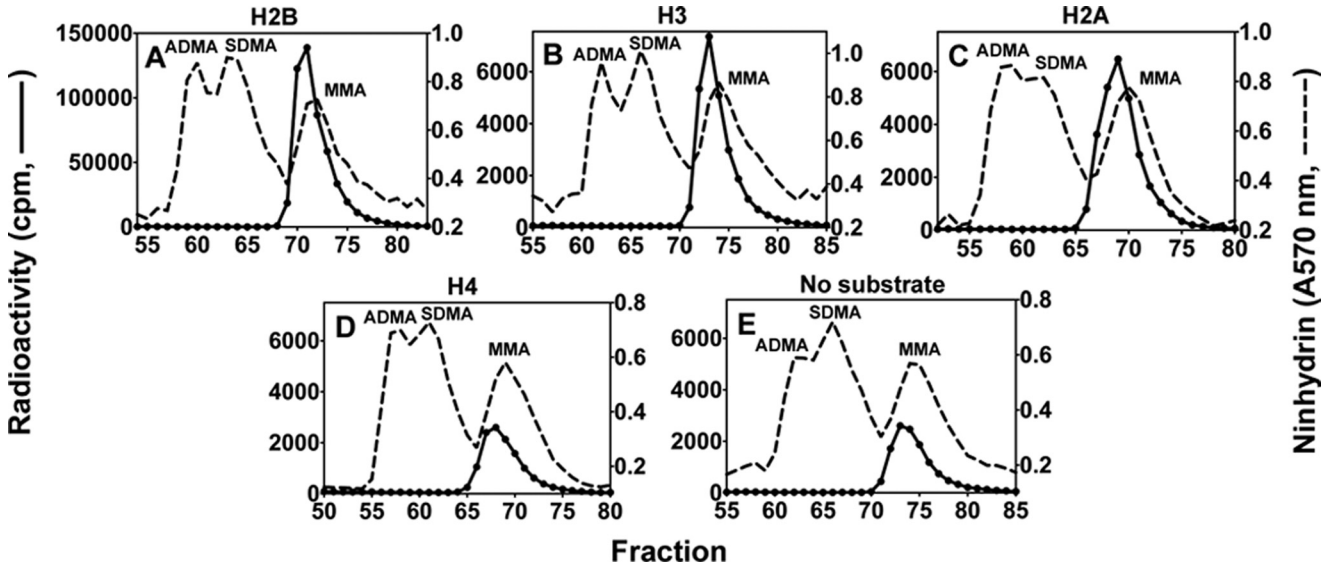

FIGURE 6. **Amino acid analysis of histones methylated by PRMT7.** 6 μg of recombinant human H2A, H2B, H3.3, or H4 was dialyzed against the reaction buffer and then incubated for 20 h with [^{3}H]AdoMet and PRMT7 (0.26 μM final concentration), hydrolyzed to amino acids, and analyzed by high resolution cation exchange chromatography as described in Fig. 2 legend. *A–D* show the PRMT7-catalyzed methylation products of H2B, H3.3, H2A, and H4. *E* shows the control of PRMT7 automethylation in the absence of histone substrates.

tion cation exchange chromatography, we were able to clearly separate MMA, SDMA, and ADMA and capture femtomole levels of methylation products from [^{3}H]AdoMet. In Fig. 3, we demonstrate the high catalytic activity of PRMT7 on GST-GAR, resulting in a peak radioactivity of $\sim 8 \times 10^4$ cpm in MMA with no SDMA or ADMA formation detected. The activity of this enzyme was about 18-fold greater than that of the GST fusion protein expressed in bacterial cells (5) when tested under similar conditions. The catalytic mutant PRMT7 retained only ~2% of this activity, confirming the absence of other PRMT enzymes in the preparation (Fig. 3*A*). Interestingly, PRMT7 alone showed relatively weak automethylation activity (a peak of $\sim 2.6 \times 10^3$ cpm), which has not been previously observed (Fig. 3*B*).

To confirm the catalytic activity forming only MMA, we compared the methylation products of a synthetic peptide based on residues 1–21 of human histone H4 along with its Arg-3 to Lys and Arg-3 to MMA derivatives (Table 1) catalyzed by PRMT7 with those catalyzed by the representative type I PRMT1 and type II PRMT5 enzymes. As shown in Fig. 4, PRMT1 formed ADMA and MMA on H4(1–21) as expected. When Arg-3 was replaced with Lys on the peptide, there was still residual activity left (~7%), indicating that Arg-17 and/or Arg-19 can also be weakly methylated by PRMT1. When the Arg-3-monomethylated peptide was used as a substrate, PRMT1 formed mainly ADMA, most likely on Arg-3, which confirms the major methylation site on the histone H4 N-terminal tail for PRMT1 (28). PRMT5 formed SDMA and MMA on H4(1–21) as expected (29). PRMT5 also showed weak activity (~20%) on the R3K mutant peptide, suggesting that Arg-17 and/or Arg-19 are its target sites as well. When Arg-3 is pre-monomethylated, PRMT5 formed mainly SDMA on H4(1–21)R3MMA, indicating Arg-3 as its major methylation site on H4 tail. Most interestingly, PRMT7 mediated formation of only MMA on all of the three H4 peptides, whether Arg-3 was mutated to Lys or MMA. These results indicate first, when there is already a methyl group on Arg-3, that PRMT7 does not add a second methyl group to it like PRMT1 and PRMT5; and second, on the H4 N-terminal tail, Arg-17 and/or Arg-19 are likely the major targets for PRMT7 rather than Arg-3.

PRMT7 Preferentially Methylates H2B among Core Histones—To study the substrate specificity of the PRMT7 enzyme expressed in insect cells, we compared the methylation level of all four core human recombinant histones catalyzed by PRMT7 in the presence of [^{3}H]AdoMet in an SDS-PAGE fluorography assay. As shown in Fig. 5, H2B was found to be a much better substrate than any of the other histones. After a 3-h exposure of the EN3HANCE^{TM} gel, only H2B appeared to be significantly methylated; after a 7-day exposure, the H2B band saturated the film response, and H2A, H3, and H4 bands became apparent. Of note, we found that replacing the histone storage buffer (300 mM NaCl, 1 mM EDTA, and 20 mM sodium phosphate, pH 7.0) with the reaction buffer (50 mM potassium HEPES, pH 7.5, 10 mM NaCl, and 1 mM DTT) significantly promoted the methylation of histone H2B, especially histones H3 and H4.

The specificity of PRMT7 for histone H2B was confirmed by amino acid analysis of the reaction products. Here, we observed a peak radioactivity of MMA of $\sim 1.4 \times 10^5$ cpm for H2B and 5% or less of this value for H2A, H3, and H4 (Fig. 6). No ADMA or SDMA products were observed in any of these reactions.

PRMT7 Targets Arg-29, Arg-31, and Arg-33 in Basic RXR Motifs on Histone H2B—Next, we aimed to identify the methylation sites of PRMT7 on H2B. First, high resolution top-down Fourier transform-MS analysis was conducted for intact H2B protein (Fig. 7*A*) and the product of H2B methylation with PRMT7 and AdoMet (Fig. 7*B*). Samples were subjected to LTQ-Orbitrap coupled with ETD, enabling us to confirm the monomethylation on H2B (Δm = 14 Da for monoisotopic mass) and selectively isolate and fragment the monomethylated species. Fig. 7*B* shows PRMT7-mediated production of a 20-charge monomethylated precursor ion ($\Delta m/z$ = 0.7 compared with the unmodified ion peak), which generated the

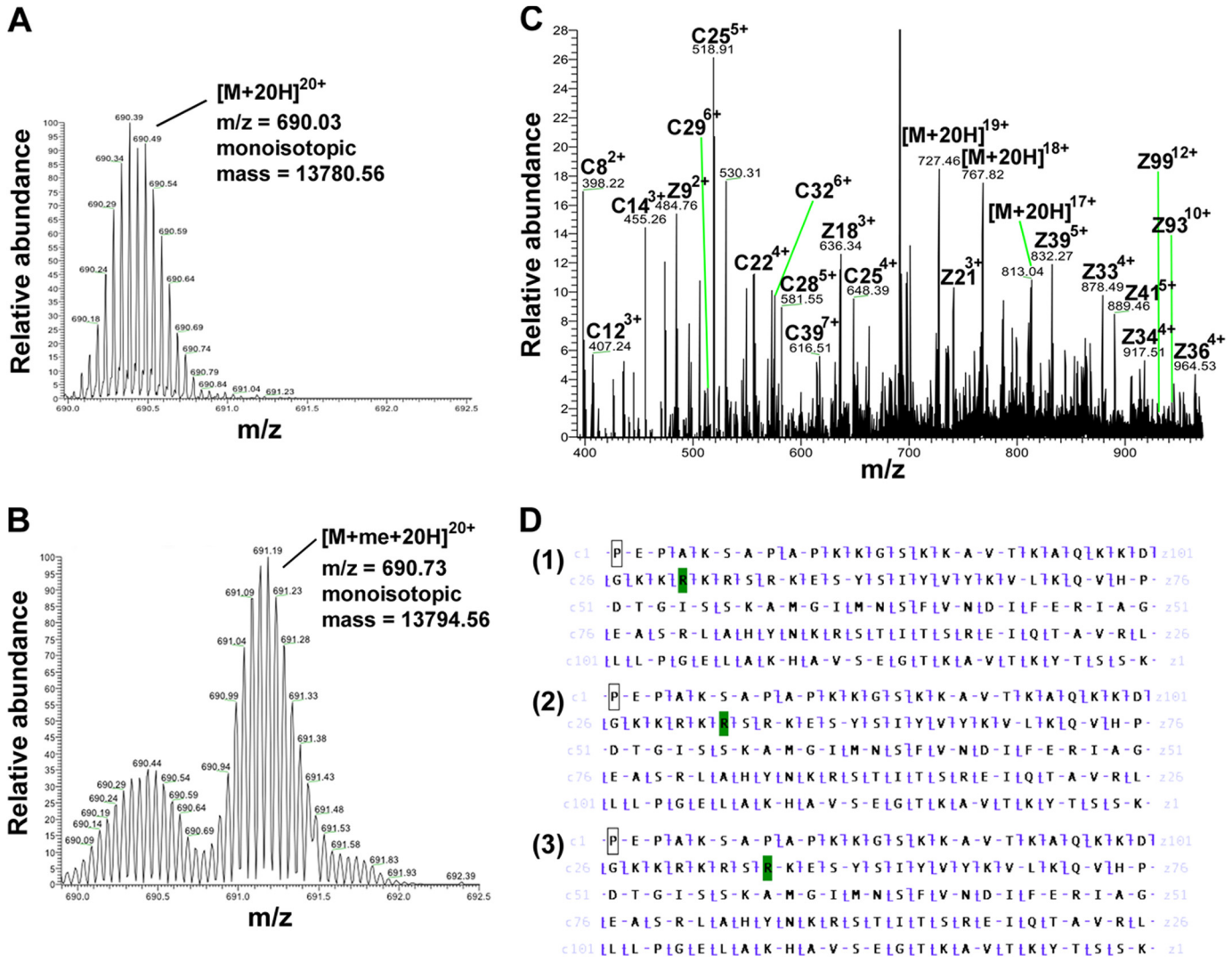

FIGURE 7. **Detection of PRMT7-formed monomethylarginine sites in histone H2B using top-down mass spectrometry.** 15 μg of H2B was incubated with 4.8 μg of PRMT7 (1 μM) and 200 μM AdoMet in the reaction buffer at room temperature for 24 h in a final volume of 60 μl. The methylation products were desalted using an OMIX C18 ZipTip and directly introduced into an LTQ-Orbitrap mass spectrometer by nano-ESI as described previously (30). *A,* control mass spectrum of unreacted H2B is shown with ion isolation of the 20-charge species (m/z = 690.03, monoisotopic mass = 13,780.56 Da; calculated monoisotopic mass 13,780.54 Da). *B,* mass spectrum of methylated H2B from the incubation mixture described above is shown with ion isolation of the 20-charge species (m/z = 690.73, monoisotopic mass = 13,794.56 Da; calculated monoisotopic mass 13,794.56 Da). *C,* ETD tandem mass spectrum of the 20-charge precursor of methylated H2B. Unit resolution was achieved on all product ions by operating the instrument at 30,000 resolution (at 400 m/z). To maximize signal intensity for better sequence coverage in the dissociation experiment, the ion isolation experimental window was kept wide enough that there was some contamination of the desired molecular ion with unmethylated H2B. The c and z ions were assigned assuming the methyl group is on H2B R29, as in panel D-1. *D,* c and z ion coverage for H2B when a methyl group is assigned on Arg-29 (D-1), Arg-R31 (D-2), or Arg-33 (D-3). The identified c and z ions are shown mapped onto the primary sequence (c ions of N-terminal origin are indicated by the *slash pointing up* and to the *left*; c ions, of C-terminal origin are indicated with a *slash pointing down* and to the *right*). In D-1, the presence of C29 and Z97 ions indicates the methylation of Arg-29. In D-2, the presence of C31 and Z97 ions indicates the methylation of either Arg-29 or Arg-31. In D-3, the presence of C34 and Z97 ions indicates the methylation of Arg-29, Arg-31, or Arg-33. Residues highlighted in *green* represent monomethylarginine sites.

product ions shown in Fig. 7*C* using ETD. The best matches for the fragment c and z ions were found for histone H2B monomethylated on either Arg-29, Arg-31, or Arg-33 (Fig. 7*D*). Analyses of other charge states of the methylated H2B also confirmed the same results. It is difficult at this point to distinguish between these three sites of methylation, although the presence of specific C29 and Z97 ions in Fig. 7*D* supports the presence of MMA at least at Arg-29. Nevertheless, it is clear that all of these sites are within the HBR region in the sequence KKRKRSRK.

To specifically map the PRMT7-catalyzed methylation sites in the N-terminal basic region of histone H2B, we prepared six peptides corresponding to residues 23–37 and containing 0, 1, or 2 Arg to Lys substitutions at Arg-29, Arg-31, and Arg-33 (Table 1). As shown in Fig. 8*A*, the wild-type peptide with three arginine residues was an excellent substrate for PRMT7 ($\sim 3 \times 10^5$ cpm in the MMA peak), confirming the results of the top-down mass spectrometry. When Arg-29 or Arg-33 was replaced, leaving R*X*R sequences, the peptides remained good substrates with 69 and 26% of the methyl-accepting activity of the wild-type peptide, respectively (Fig. 8, *C* and *D*). However, when the central Arg-31 residue was replaced, the methyl-accepting activity decreased to only ~3% of the wild-type peptide (Fig. 8*E*). More interestingly, when two of the three arginine residues were replaced by lysine residues, leaving only a single

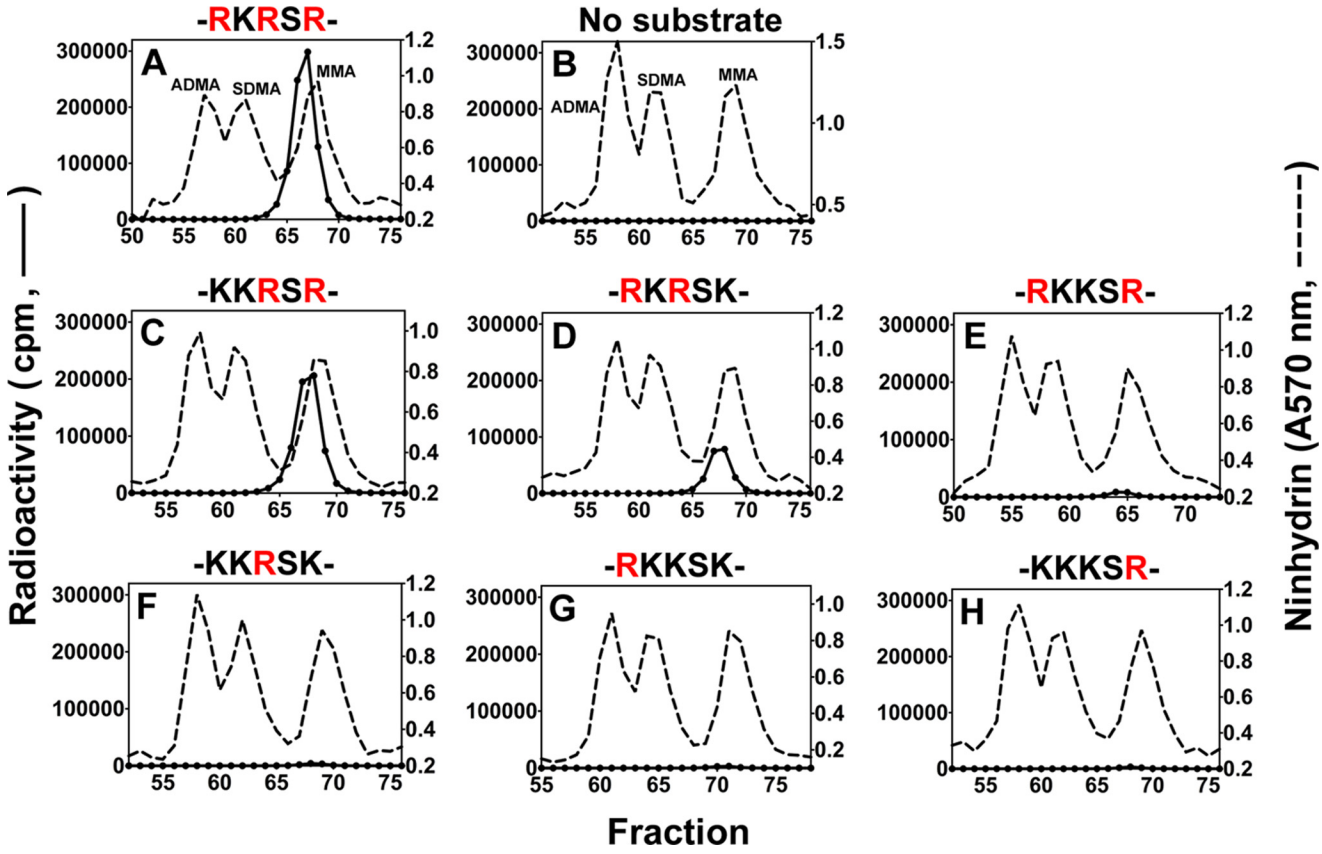

FIGURE 8. **Amino acid analysis of peptides derived from residues 23–37 of histone H2B methylated by PRMT7.** Peptides (12.5 μM final concentration; Table 1) were methylated by PRMT7 as described in Fig. 3 legend. *A–H* show PRMT7-catalyzed methylation products of H2B(23–37), no substrate, H2B(23–37)R29K, H2B(23–37)R33K, H2B(23–37)R31K, H2B(23–37)R29K,R33K, H2B(23–37)R31K,R33K, and H2B(23–37)R29K,R31K, respectively. Partial sequences containing the target arginine sites and their lysine mutations are indicated *above* the panels. The arginine methylation sites present in each peptide are highlighted in *red*.

arginine residue at positions 29, 31, or 33, the methyl-accepting activity dropped to only ~1% of the wild-type peptide (Fig. 8, *F–H*). These latter activities were only 3–4 times higher than the background MMA level formed by automethylation of PRMT7 under the same conditions (Fig. 8*B*). These data indicate that PRMT7 can monomethylate any of the three arginine residues in this region but that it shows a dramatically higher activity when at least two arginine residues are present and spaced with only one residue between them, suggesting a preferred R*X*R substrate recognition motif for PRMT7.

The k_{cat} and K_m values for selected H2B peptides containing the RKRKR sequence and its variants are shown in Table 2. Here, the value of the k_{cat}/K_m is about 4–29-fold lower when either terminal arginine residue is replaced by a lysine residue. When the central arginine residue is replaced by a lysine residue to eliminate the R*X*R motif, the k_{cat} value is over 50-fold lower, and the activity is too low to obtain a reliable K_m value. When these values are compared with those of other mammalian PRMTs reported in the literature, the k_{cat}/K_m value for PRMT7 is some 10–1000-fold lower than those for PRMT1, and -3–6, but similar to that of PRMT8 and some 50-fold greater than that of PRMT2. Although these values were determined using differing experimental conditions and substrates, it appears that there is a wide range of activity for mammalian PRMTs.

Finally, to pin down the localization of the methylation sites, we performed high resolution tandem MS analyses of the methylated wild-type H2B(23–37) peptide and its R29K mutant. Fig. 9*A* shows an example of the 5-charge state of H2B(23–37) with an m/z of 388.03, which was deconvoluted to the monoisotopic mass of the peptide (1935.12 Da). After the reaction was catalyzed by PRMT7, Fig. 9*B* shows the generation of singly, doubly, and triply methylated H2B(23–37) (m/z = 390.83, 393.63, and 396.43 and monoisotopic mass = 1949.13, 1963.14, and 1977.15 Da, respectively), with ~60% of singly methylated products, indicating the high conversion but low processivity of PRMT7 under our experimental conditions. As the amino acid analysis showed that all the methylated arginines were monomethylated (Fig. 8), the existence of triply methylated peptide confirms that all three arginines in H2B(23–37) can be methylated, although the chance of adding three methyl groups was very low. The singly methylated precursor ion generated the product ions in Fig. 9*C*, giving the best c and z ion coverage of the H2B(23–37) sequence when the methyl group was assigned to Arg-29, Arg-31, or Arg-33 (Fig. 9*D*). The c and z ions in D-1 and D-2 strongly suggested methylation of Arg-29 and Arg-31; those in D-3 did not support but could not exclude the methylation of Arg-33, probably because Arg-33 was methylated to a very low level. Thus, the singly methylated species was actually a mixture of peptides

TABLE 2

Comparison of kinetic parameters of PRMT7 with other mammalian PRMTs

Values of k_{cat} and K_m of PRMT7 were measured as described previously (26). Varied concentrations of the indicated H2B peptides (0–100 μM) were mixed with 0.1 μM PRMT7 and 10 μM *S*-adenosyl-[*methyl*-^{14}C]L-methionine (47 mCi/mmol, PerkinElmer Life Sciences) in 50 mM potassium HEPES, pH 7.5, 10 mM NaCl, 1 mM DTT, and 20 μM sodium EDTA, and incubated at room temperature for 4–5 h. Duplicate reactions mixtures were spotted onto Whatman P81 filters that were washed extensively in 50 mM $NaHCO_3$, pH 9, and counted by liquid scintillation as described previously (26). Data were analyzed by a nonlinear fit to the Michaelis-Menten equation using GraphPad Prism software; ± values reflect the standard error.

Enzyme (Ref.)	Substrate	k_{cat}	K_m (methyl-accepting substrate)	k_{cat}/K_m
		h^{-1}	μM	$\mu M^{-1}\,h^{-1}$
PRMT1 (26)	H4 (1–20)	38.4	0.34	106.8
PRMT1 (31)	H4 (1–21)	27.6	1.1	25.1
PRMT1 (32)	H4 protein	5.0	4.2	1.2
PRMT2 (32)	H4 protein	0.0065	3.3	0.0020
PRMT3 (33)	Ribosomal protein S2	6	1	6
PRMT4 (34)	H3 protein	25	≤0.2	≥50
PRMT5/MEP50 (26)	H4 (1–20)	2.6	0.63	4.1
PRMT6 (35)	H4 (1–21)	9.6	5.5	1.7
PRMT7 (this study)	H2B (23–37)	0.62 ± 0.02	6.9 ± 0.5	0.090 ± 0.007
PRMT7 (this study)	H2B (23–37)R29K	0.26 ± 0.01	11.0 ± 1.1	0.024 ± 0.003
PRMT7 (this study)	H2B (23–37)R31K	0.011 ± 0.002	[a]	
PRMT7 (this study)	H2B (23–37)R33K	0.094 ± 0.010	30.5 ± 7.7	0.0031 ± 0.0008
PRMT8 (36)	H4 protein	0.14	1.5	0.096

[a] Data values were too low for accurate determination.

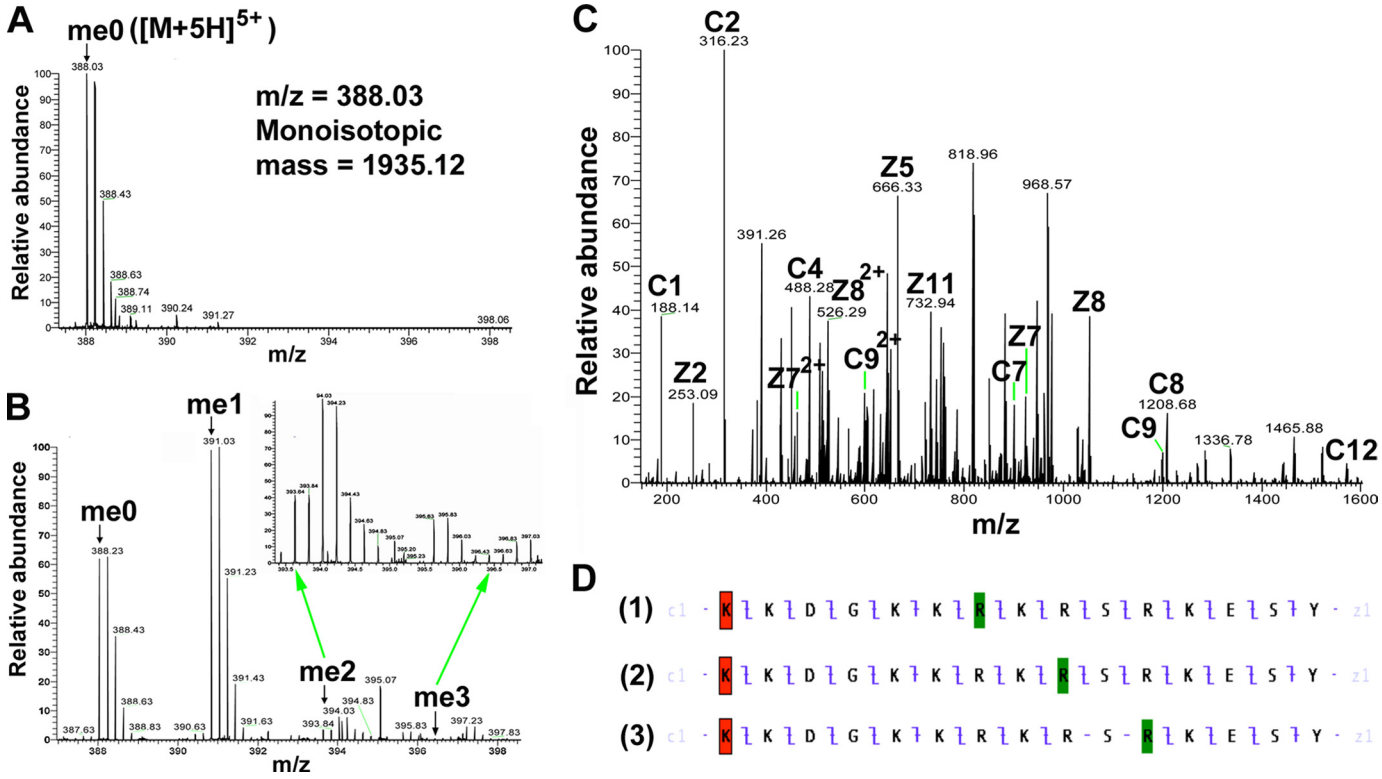

FIGURE 9. **Detection of PRMT7-formed monomethylarginine sites in a peptide corresponding to residues 23–37 of histone H2B by mass spectrometry.** 24 μM H2B(23–37) was incubated with 4.8 μg of PRMT7 (1.87 μM) and AdoMet (182 μM) in reaction buffer in a final volume of 33 μl at room temperature for 24 h. The methylation products were desalted with OMIX C18 ZipTip and directly introduced into an LTQ-Orbitrap mass spectrometer by nano-ESI, as in Fig. 6. *A,* control mass spectrum showing the +5 charged state of unmethylated H2B(23–37) (**me0**; *m/z* = 388.03, monoisotopic mass = 1935.11 Da; calculated monoisotopic mass = 1935.12 Da). *B,* LTQ-Orbitrap spectrum showing the +5 charged state of PRMT7-methylated H2B(23–37). The species detected included the unmethylated (**me0**), the monomethylated (**me1**; *m/z* = 390.83, monoisotopic mass = 1949.13 Da; calculated monoisotopic mass = 1949.14 Da), the doubly methylated (**me2**; *m/z* = 393.63, monoisotopic mass = 1963.14 Da; calculated monoisotopic mass = 1963.15 Da), and the triply methylated (**me3**; *m/z* = 396.43, monoisotopic mass = 1977.15 Da; calculated monoisotopic mass = 1977. 17 Da). The *inset* shows a magnification of the region for doubly and triply methylated H2B(23–37). *C,* ETD tandem mass spectrum of the 5-charge precursor of monomethylated H2B(23–37). The peaks corresponding to **me1** in *B* were isolated and fragmented with ETD. Unit resolution was achieved on all product ions by operating the instrument at 60,000 resolution (at 400 *m/z*). Note that **me1** is a mixture of Arg-29-methylated, Arg-31-methylated, and Arg-33-methylated species. The c and z ions were assigned assuming the methyl group is on Arg-31, as in panel D-2. *D,* c and z ion coverage for H2B(23–37) peptide when a methyl group is assigned on Arg-29 (D-1), Arg-31 (D-2), or Arg-33 (D-3). In D-1, the presence of C7 and Z9 ions indicates the monomethylation of Arg-29. In D-2, the presence of C9 and Z7 ions indicates the monomethylation of Arg-31. In D-3, the Z5 and Z6 ions supporting monomethylation of Arg-33 were not found, probably because Arg-33 is methylated to a very low extent, as suggested by *B* **me3**. Acetylation of the N-terminal lysine residue is indicated by *red shading*; monomethylation of arginine residues is indicated by *green shading*.

with monomethylation on different arginine residues, and Arg-29 and Arg-31 should be the major methylation sites on H2B. Additionally, the fragmentation pattern for the methylated H2B(23–37)R29K peptide is more consistent with the Arg-31 site of methylation (Fig. 10). Combined with the presence of a small amount of dimethylated peptide, these

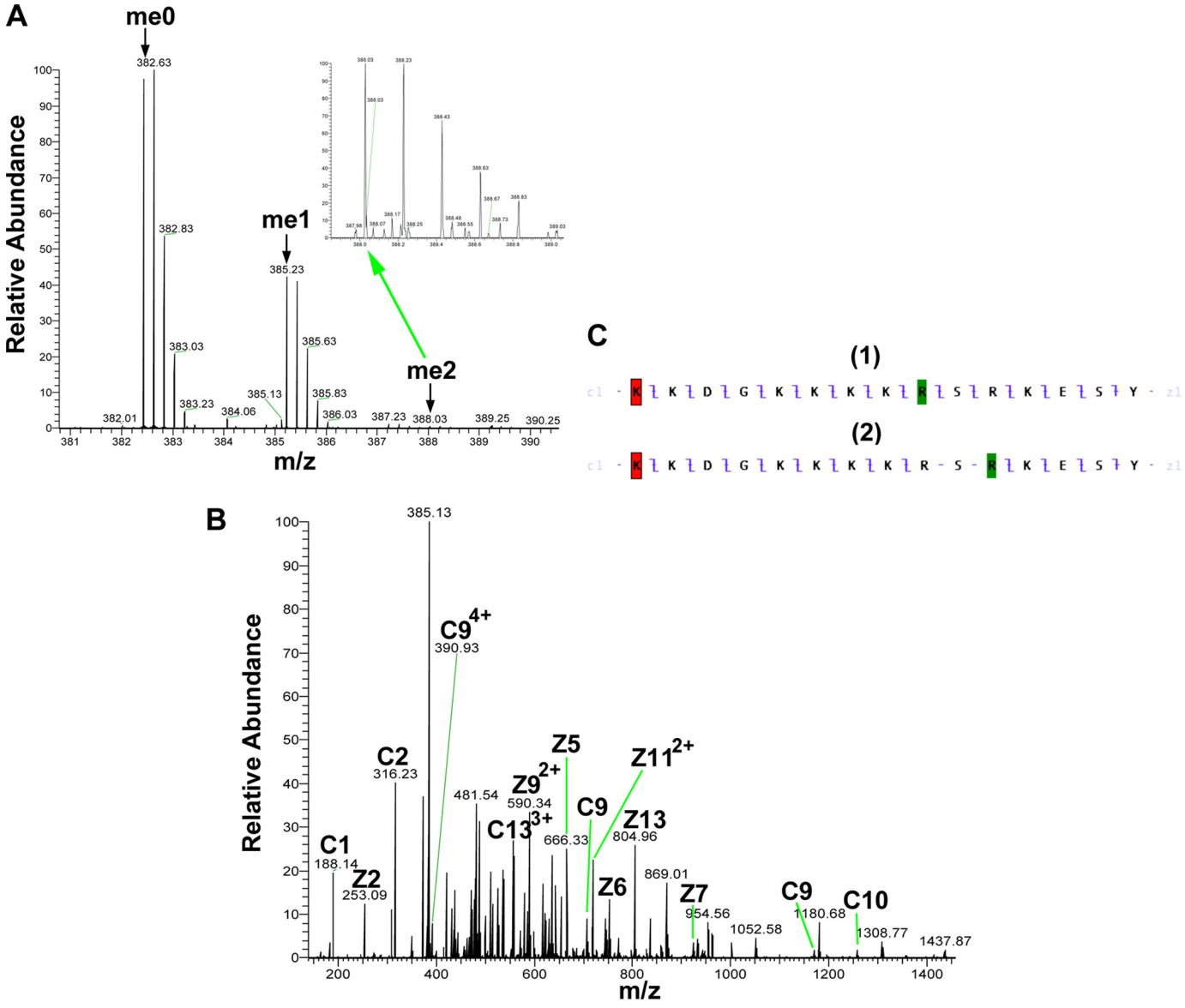

FIGURE 10. **Detection of PRMT7-formed monomethylarginine sites in a peptide corresponding to residues 23–37 of histone H2B with Arg-29 to Lys mutation by mass spectrometry.** 24 μM H2B(23–37)R29K was incubated with 4.8 μg of PRMT7 (1.87 μM) and AdoMet (182 μM) in the reaction buffer in a final volume of 33 μl at room temperature for 24 h. The methylation products were desalted with OMIX C18 ZipTip and directly introduced into an LTQ-Orbitrap mass spectrometer by nano-ESI as described above. *A,* mass spectrum showing the +5 charged state of PRMT7-methylated H2B(23–37)R29K. The species detected included the unmethylated (***me0***; m/z = 382.43, monoisotopic mass = 1907.11 Da; calculated monoisotopic mass = 1907.11 Da), the monomethylated (***me1***; m/z = 385.23, monoisotopic mass = 1921.12 Da; calculated monoisotopic mass = 1921.13 Da), doubly methylated (***me2***; m/z = 388.03, monoisotopic mass = 1935.11 Da; calculated monoisotopic mass = 1935.15 Da). The *inset* shows a magnification of the region for doubly methylated H2B(23–37)R29K. *B,* ETD tandem mass spectrum of the 5-charge precursor of monomethylated H2B(23–37)R29K. The peaks corresponding to ***me1*** in *A* were isolated and fragmented with ETD. The c and z ions were assigned assuming the methyl group is on Arg-31, as in *C-1*. *C,* c and z ion coverage for H2B(23–37)R29K when a methyl group is assigned on Arg-31 (B-1) or Arg-33 (B-2). In *C-1*, the presence of C9 and Z7 ions indicates the monomethylation of Arg-31. *C-2*, the Z5 and Z6 ions supporting monomethylation of R33 were not found, probably because Arg-33 is methylated to a very low extent, as suggested in *A,* ***me2***. Acetylation of the N-terminal lysine residue is indicated by *red shading*; monomethylation of arginine residues is indicated by *green shading*.

results also suggest that Arg-31 is a major site of methylation, and Arg-33 is a minor site.

Confirmation of the RXR Recognition Motif for PRMT7 Using Histone H4 N-terminal Peptides—Although the recombinant histone H4 protein did not appear to be a good substrate for PRMT7 (Fig. 6*D*), the H4(1–21) peptide was well methylated (Fig. 4*G*). To identify the methylation sites on H4 N-terminal tail, short H4 peptides were synthesized covering the 1–8 or 14–22 residues, and the Arg-17/Arg-19 to Lys derivatives were also made for the latter peptide. As shown in Fig. 11, H4(14–22) could still be methylated by PRMT7 ($\sim 4 \times 10^3$ cpm in the MMA peak), but the activity was much weaker compared with H4(1–21) (Fig. 4*G*, $\sim 8 \times 10^4$ cpm in the MMA peak), indicating that distant residues on the H4 N terminus also play a role in substrate recognition. Surprisingly, comparing Fig. 11, *B* and *C,* with *E,* the methyl-accepting activity of H4(14–22)R17K or R19K for PRMT7 was not much greater than PRMT7 automethylation (Fig. 11*E*). These results show again that a single arginine residue, even within a basic residue context, is not a good target for PRMT7. Consistent with this idea, the H4(1–8) peptide, containing a single arginine residue at position 3 that is a substrate for both PRMT1 and PRMT5 (28, 29), was not

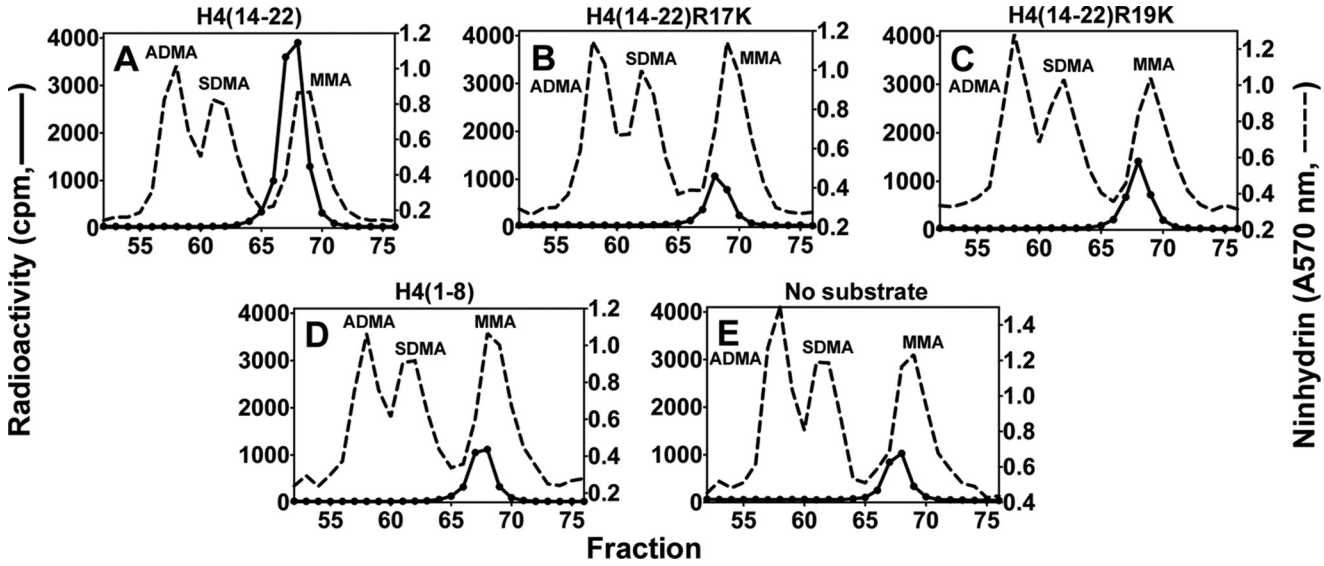

FIGURE 11. **Amino acid analysis of peptides derived from residues 14–22 of histone H4 methylated by PRMT7.** Peptides (12.5 μM; Table 1) were incubated with PRMT7 (0.26 μM) and [^{3}H]AdoMet (0.7 μM) as described under "Experimental Procedures," and the reactions were allowed to proceed at room temperature for 20 h. The reaction mixtures were then acid-hydrolyzed and analyzed for methylated arginine species as described. *A–D* show PRMT7-catalyzed methylation products of H4(14–22), H4(14–22)R17K, H4(14–22)R19K, and H4(1–8), respectively. *E* shows the control of PRMT7 automethylation.

detected as a substrate for PRMT7 (compare Fig. 11, *D* with *E*). Finally, tandem MS analysis of the PRMT7 methylated H4(1–21) peptide also suggested the absence of methylation at Arg-3 and the presence of methylation at Arg-17 and Arg-19 (Fig. 12). The 5-charge state of unmethylated H4(1–21) showed an m/z of 427.46, deconvoluting to a monoisotopic mass of 2132.26 Da. After the PRMT7-catalyzed reaction, the singly methylated peptide (m/z = 430.26, monoisotopic mass = 2146.27 Da) and doubly methylated peptide (m/z = 433.06, monoisotopic mass = 2160.28 Da) were also present, although the level for the latter was very low. ETD fragmentation gave informative c and z ions covering most of H4(1–21) sequence when a methyl group was assigned on Arg-17 (Fig. 12*D*) (2). But C17, C18 and Z3, Z4 ions were missed if a methyl group was assigned on Arg-19 (Fig. 12*D* (3)), indicating it was less strongly methylated. Putting a methyl group on Arg-3 significantly lowered the sequence coverage (Fig. 12*D*) (1), suggesting H4R3 was not likely the methylation site. Together, the MS data gave evidence for methylation of H4R17 and Arg-19 by PRMT7, with a preference for Arg-17.

DISCUSSION

We have shown that an insect cell-expressed mouse PRMT7 has a robust protein arginine methyltransferase activity, but one that is limited to the formation of MMA residues within specific R*X*R motifs. These results support the assignment of a type III activity to this enzyme that was previously observed for a GST-tagged PRMT7 expressed in bacteria (4, 5) and that is consistent with the type III assignment for the worm (17) and trypanosome (18) homologs. It is not clear at this point what contributes to the enhanced activity of the insect cell-expressed enzyme, although it is possible that insect cell post-translational modifications and differences in the N- and C-terminal tags can affect the activity. Initial mass spectrometric analysis of tryptic peptides of PRMT7 suggested possible sites of phosphorylation and methylation, but these results need to be verified. However, this analysis demonstrated no contamination of the insect cell-expressed enzyme with other methyltransferases.

Previous results suggesting that PRMT7 has the ability to form ADMA and/or SDMA (9, 16, 20) may have been compromised by contamination of enzyme preparations with other PRMTs, particularly when FLAG-tagged PRMT7 is purified in a protocol also known to purify nontagged PRMT5 (2, 3, 5, 19). Endogenous PRMT5 in mammalian cells has an affinity for the monoclonal M2 antibody used to purify FLAG-tagged proteins (19). As such, nontagged PRMT5 can be co-purified with FLAG-PRMT7, and the methyltransferase activity detected from such preparations would be from the mixture of both enzymes, leading to misidentification of SDMA generated by PRMT5 as a PRMT7 product. For example, the observation of methylation in peptide sites corresponding to Arg-3 of histone H2A and H4 (9) may be due to PRMT5 rather than PRMT7, especially because these sites are known substrates of PRMT5 (2, 26). Additionally, the reported methylation of Arg-3 on recombinant histone H4 and R2 on histone H3 (20) may also be due to PRMT5 contamination. The distinct preference of PRMT5 for Arg-3 and PRMT7 for Arg-17/Arg-19 in H4(1–21) is clearly shown in Fig. 4. Because the activity of PRMT5 is ~45 times greater than that of PRMT7 (Table 2), a small degree of contamination with PRMT5 can mask the activity of PRMT7. The very high relative activity of PRMT1 (Table 2) may also lead to misleading results if PRMT7 preparations are contaminated with this enzyme. Finally, we note that the H4(1–21) and H4(1–21)R3K peptides can be effectively used to distinguish PRMT7 activity from that of PRMT5 and PRMT1 as demonstrated in Fig. 4.

We have shown that PRMT7 automethylation occurs in the insect cell-expressed enzyme; such an automethylation activity can complicate substrate identification and necessitates enzyme-only controls. Automethylation has been previously observed in several other methyltransferases (37) and has

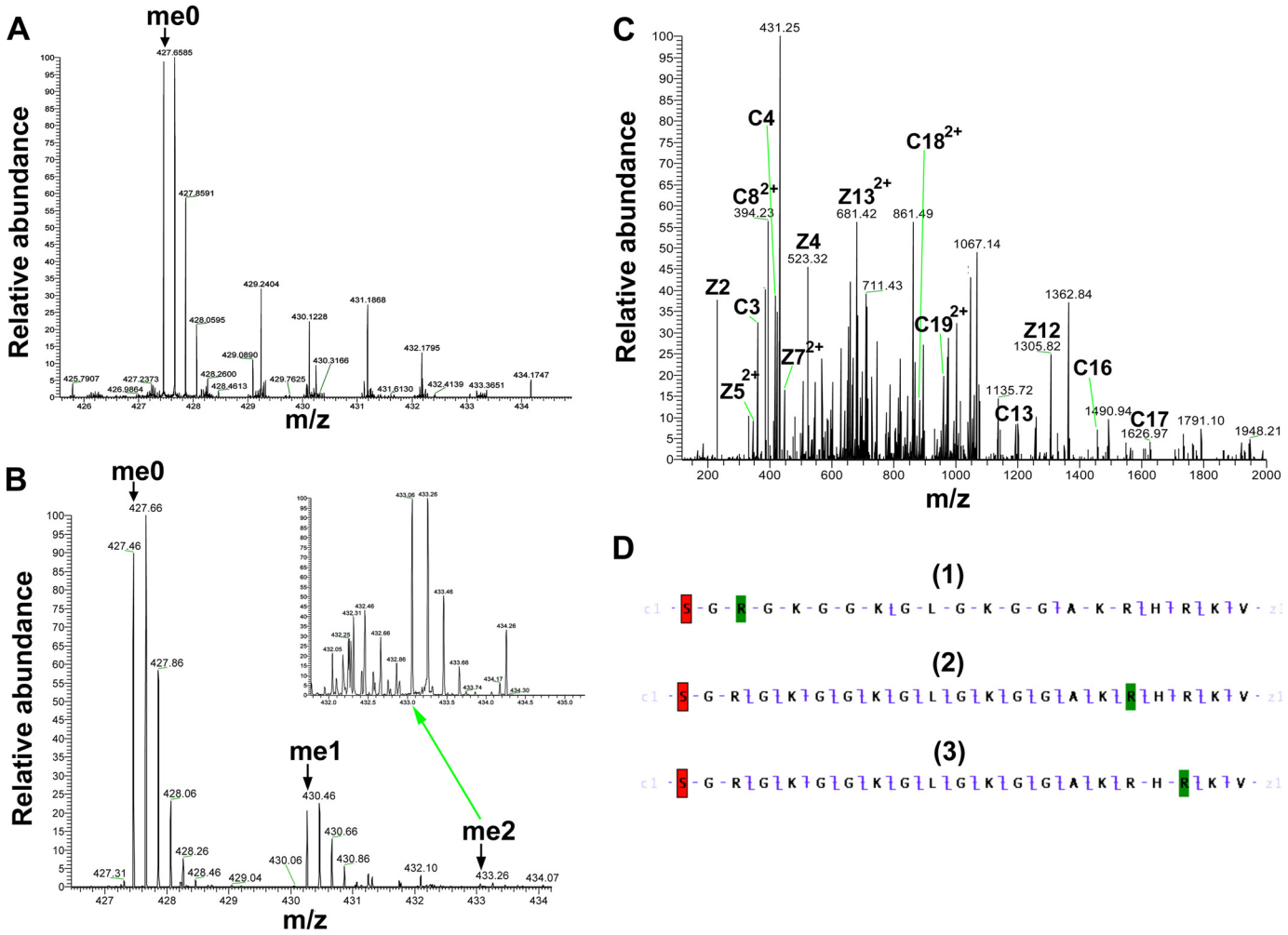

FIGURE 12. **Detection of PRMT7-formed monomethylarginine sites in a peptide corresponding to residues 1–21 of histone H4 by mass spectrometry.** 24 μM H4(1–21) was incubated with 4.8 μg of PRMT7 (1.87 μM) and AdoMet (182 μM) in the reaction buffer in a final volume of 33 μl at room temperature for 24 h. The methylation products were desalted with OMIX C18 ZipTip and directly introduced into an LTQ-Orbitrap mass spectrometer by nano-ESI as described above. *A,* control mass spectrum showing the +5 charged state of unmethylated H4(1–21) (***me0***; m/z = 427.46, monoisotopic mass = 2132.25 Da; calculated monoisotopic mass = 2132.26 Da). *B,* mass spectrum showing the +5 charged state of PRMT7-methylated H4(1–21). The species detected included the unmethylated (***me0***), the monomethylated (***me1***; m/z = 430.26, monoisotopic mass = 2146.27 Da; calculated monoisotopic mass = 2146.27 Da), the doubly methylated (***me2***; m/z = 433.06, monoisotopic mass = 2160.26 Da; calculated monoisotopic mass = 2160.29 Da). The *inset* shows a magnification of the region for doubly methylated H4(1–21). *C,* ETD tandem mass spectrum of the 5-charge precursor of monomethylated H4(1–21). The peaks corresponding to ***me1*** in *B* were isolated and fragmented with ETD. The c and z ions were assigned assuming the methyl group is on Arg-17, as in D-2. *D,* c and z ion coverage for H4(1–21) when a methyl group is assigned on Arg-3 (*D-1*), Arg-17 (*D-2*), or Arg-19 (*D-3*). D-1, the absence of majority of ions indicates that H4R3 is not a good methylation site for PRMT7. D-2, the presence of C17 and Z5 ions indicates monomethylation of Arg-17. D-3, the presence of C19 and Z5 ions indicates monomethylation of Arg-17 or Arg-19. Acetylation of the N-terminal lysine residue is indicated by *red shading*; monomethylation of arginine residues is indicated by *green shading*.

been associated with the regulation of activity in CARM1/PRMT4 (38).

The substrate specificity of PRMTs has been reviewed by Yang and Bedford (3). Most PRMTs, including PRMT1, -3, -6, and -8, target glycine- and arginine-rich motifs, which are involved in mediating nucleic acid and protein interactions (39, 40); CARM1/PRMT4 specifically methylates proline-, glycine-, and methionine-rich motifs (41), although PRMT5 works on both (41, 42). Adding to this substrate profile, we now demonstrate that PRMT7 shows a unique substrate specificity that is distinct from other known PRMT members. PRMT7 methylates two very basic regions on the H2B protein and peptides and H4 peptides where two or more closely positioned arginine residues are present in sequences rich in lysine residues. The mutation analyses on peptides H2B(23–37) and H4(14–22) also suggest that PRMT7 strongly prefers two arginines with one residue apart to a single arginine or two arginines with three residues apart, even if they are located in the same basic region. These results lead us to propose that PRMT7 specifically recognizes lysine- and arginine-rich (KAR) regions with an R*X*R motif. The binding selectivity for arginine over lysine is significant despite their similar chemical nature, as replacing one of the arginines with lysine decreases the methylation efficiency.

PRMT7 methylates the four core histones to different extents with a clear preference for the N-terminal basic motif of H2B. The very high methyl-accepting activity of H2B *in vitro* suggests that it might be a physiological substrate for PRMT7. Previous studies identified multiple post-translational modifications on human H2B, including acetylation on Lys-5, Lys-15,

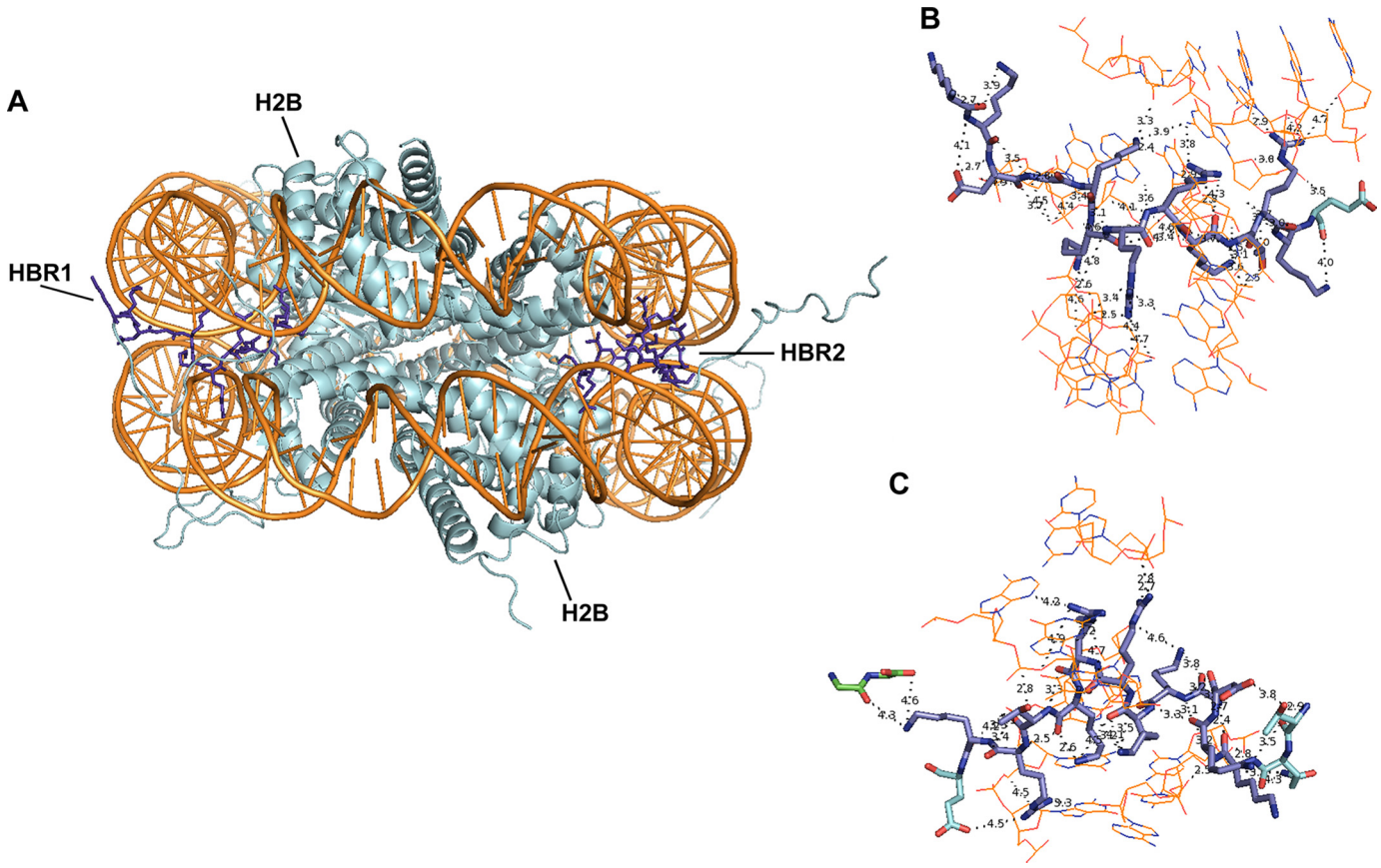

FIGURE 13. **Crystal structure of H2B N-terminal basic regions in a nucleosome core particle (Protein Data Bank code 1KX5, 1.9-Å resolution).** *A,* two molecules of histone H2B.2 (*Xenopus laevis*; *cyan*) from a histone octamer wrapped by two strands of nucleosomal DNA (*Homo sapiens*; *orange*). The H2B repression region (*HBR*; sequence, KKDGKKRRKTRK; residues highlighted as *blue sticks*) is at the root of the flexible N-terminal tail and exits the nucleosome through a minor groove channel formed by two DNA strands (1). *B* and *C* exhibit magnifications of HBR1 and HBR2 areas from *A*. They are both tightly associated with surrounding DNA. Noncovalent bonds with distance <5 Å are shown. *Green,* Gly-101 and Gly-102 are from histone H4.

Lys-16, and Lys-20 (43, 44), phosphorylation on Ser-14 (45), and methylation on Lys-46, Lys-57, and Lys-108 (43). However, arginine methylation on HBR has not been reported to our knowledge. These MMA modifications may have been missed because traditional tryptic digestion in bottom-up mass spectrometric analysis may cleave KAR regions like the methylated sequence -KKRKRSRK- in histone H2B into small fragments that are undetectable for LC-MS/MS analysis. A similar situation may occur with the -KRHRK- sequence in histone H4. It is also possible that the stoichiometry of methylation of these R*X*R sites in histones H2B and H4 is very low. We have shown that the histone-histone and histone-DNA interactions both inhibit H2B methylation *in vitro*. In the nucleosome structure, the target arginine residues of histones H2B and H4 are generally bound to DNA and may be largely inaccessible to PRMT7 until a conformational change occurs. Additional studies will be required to identify these potential new methylation sites *in vivo*, as well as sites on non-histone proteins.

With the revelation of its catalytic pattern and substrate specificity, it is intriguing to speculate on the biological consequences of potential PRMT7-mediated histone methylation. For histone H4, the KRHRK region has been shown to interact with the acidic islet of the H2A globular domain and possibly Arg-96 to Leu-99 of H2B from the neighboring nucleosome and to facilitate nucleosome array compaction (46–50). The same RHR region (residues 17–19) has also been demonstrated to interact with a C-terminal acidic patch of Dot1 methyltransferase, facilitating Dot1-mediated histone H3K79 methylation and telomeric silencing (51). For histone H2B, the N-terminal HBR region KKDGKKRKRSRK associates with DNA, stabilizes nucleosome structure, and silences gene expression (52, 53). Methylation of these basic regions may compromise their interaction with protein or DNA binding partners, affecting downstream processes, including transcription (54). It is thus possible that PRMT7 modulates chromatin stability and transcription initiation. Because the PRMT7-targeting basic region is located at the end of the flexible N-terminal tail of H2B and is in close contact with negatively charged DNA chains (Fig. 13), its modification by PRMT7 may not occur, although this region is tightly bound to surrounding DNA. It is also possible that H2B is methylated before it is incorporated into the nucleosome, perhaps as a marker for histone assembly as in the case of H3K56 acetylation during replication (55). A final possibility is that once H2B dissociates out of the nucleosome, PRMT7-mediated methylation targets it for ubiquitination and then degradation, as in the case for PRMT5-catalyzed methylation on Arg-111 and Arg-113 of E2F-1 (56).

In summary, our discovery of the sequence motif for PRMT7 recognition will facilitate the identification of physiological

substrates and the effects of protein arginine methylation on their functions in health and disease.

Acknowledgments—We thank Stéphane Richard (McGill University) for valuable suggestions in initiating the project. We thank Paul Thompson and Heather Rust (Scripps Research Institute) for the gifts of His-PRMT1 and the H4(1–21), H4(1–21)R3K, and H4(1–21)R3MMA peptides. We thank Jill Butler and Sharon Dent (MD Anderson Cancer Center) for the gift of Myc-PRMT5. We thank Yan Coulombe for assistance with protein purification. LC-MS/MS analyses of tryptic peptides of PRMT7 were performed at the University of Alabama at Birmingham CCC Proteomics Core. We also thank the previous and current members of the Clarke laboratory, in particular Alexander Patananan and Jonathan Lowenson for their help.

REFERENCES

1. Walsh, C. T. (2006) *Post-translational Modification of Proteins: Expanding Nature's Inventory,* pp. 1–490, Roberts and Co. Publishers, Englewood, CO
2. Bedford, M. T., and Clarke, S. G. (2009) Protein arginine methylation in mammals: who, what, and why. *Mol. Cell* **33,** 1–13
3. Yang, Y., and Bedford, M. T. (2013) Protein-arginine methyltransferases and cancer. *Nat. Rev. Cancer* **13,** 37–50
4. Miranda, T. B., Miranda, M., Frankel, A., and Clarke, S. (2004) PRMT7 is a member of the protein arginine methyltransferase family with a distinct substrate specificity. *J. Biol. Chem.* **279,** 22902–22907
5. Zurita-Lopez, C. I., Sandberg, T., Kelly, R., and Clarke, S. G. (2012) Human protein arginine methyltransferase 7 (PRMT7) is a type III enzyme forming ω-NG-monomethylated arginine residues. *J. Biol. Chem.* **287,** 7859–7870
6. Herrmann, F., Pably, P., Eckerich, C., Bedford, M. T., and Fackelmayer, F. O. (2009) Human protein-arginine methyltransferases *in vivo*–distinct properties of eight canonical members of the PRMT family. *J. Cell Sci.* **122,** 667–677
7. Auclair, Y., and Richard, S. (2013) The role of arginine methylation in the DNA damage response. *DNA Repair* **12,** 459–465
8. Gonsalvez, G. B., Tian, L., Ospina, J. K., Boisvert, F. M., Lamond, A. I., and Matera, A. G. (2007) Two distinct arginine methyltransferases are required for biogenesis of Sm-class ribonucleoproteins. *J. Cell Biol.* **178,** 733–740
9. Karkhanis, V., Wang, L., Tae, S., Hu, Y. J., Imbalzano, A. N., and Sif, S. (2012) Protein arginine methyltransferase 7 regulates cellular response to DNA damage by methylating promoter histones H2A and H4 of the polymerase δ catalytic subunit gene, POLD1. *J. Biol. Chem.* **287,** 29801–29814
10. Buhr, N., Carapito, C., Schaeffer, C., Kieffer, E., Van Dorsselaer, A., and Viville, S. (2008) Nuclear proteome analysis of undifferentiated mouse embryonic stem and germ cells. *Electrophoresis* **29,** 2381–2390
11. Dhar, S. S., Lee, S. H., Kan, P. Y., Voigt, P., Ma, L., Shi, X., Reinberg, D., and Lee, M. G. (2012) Trans-tail regulation of MLL4-catalyzed H3K4 methylation by H4R3 symmetric dimethylation is mediated by a tandem PHD of MLL4. *Genes Dev.* **26,** 2749–2762
12. Gros, L., Renodon-Cornière, A., de Saint Vincent, B. R., Feder, M., Bujnicki, J. M., and Jacquemin-Sablon, A. (2006) Characterization of prmt7α and -β isozymes from Chinese hamster cells sensitive and resistant to topoisomerase II inhibitors. *Biochim. Biophys. Acta* **1760,** 1646–1656
13. Verbiest, V., Montaudon, D., Tautu, M. T., Moukarzel, J., Portail, J. P., Markovits, J., Robert, J., Ichas, F., and Pourquier, P. (2008) Protein arginine *N*-methyl transferase 7 (PRMT7) as a potential target for the sensitization of tumor cells to camptothecins. *FEBS Lett.* **582,** 1483–1489
14. Bleibel, W. K., Duan, S., Huang, R. S., Kistner, E. O., Shukla, S. J., Wu, X., Badner, J. A., and Dolan, M. E. (2009) Identification of genomic regions contributing to etoposide-induced cytotoxicity. *Hum. Genet.* **125,** 173–180
15. Thomassen, M., Tan, Q., and Kruse, T. A. (2009) Gene expression meta-analysis identifies chromosomal regions and candidate genes involved in breast cancer metastasis. *Breast Cancer Res. Treat.* **113,** 239–249
16. Lee, J. H., Cook, J. R., Yang, Z. H., Mirochnitchenko, O., Gunderson, S. I., Felix, A. M., Herth, N., Hoffmann, R., and Pestka, S. (2005) PRMT7, a new protein arginine methyltransferase that synthesizes symmetric dimethylarginine. *J. Biol. Chem.* **280,** 3656–3664
17. Takahashi, Y., Daitoku, H., Yokoyama, A., Nakayama, K., Kim, J. D., and Fukamizu, A. (2011) The *C. elegans* PRMT-3 possesses a type III protein arginine methyltransferase activity. *J. Recept. Signal Transduct. Res.* **31,** 168–172
18. Fisk, J. C., Sayegh, J., Zurita-Lopez, C., Menon, S., Presnyak, V., Clarke, S. G., and Read, L. K. (2009) A type III protein arginine methyltransferase from the protozoan parasite *Trypanosoma brucei*. *J. Biol. Chem.* **284,** 11590–11600
19. Nishioka, K., and Reinberg, D. (2003) Methods and tips for the purification of human histone methyltransferases. *Methods* **31,** 49–58
20. Migliori, V., Müller, J., Phalke, S., Low, D., Bezzi, M., Mok, W. C., Sahu, S. K., Gunaratne, J., Capasso, P., Bassi, C., Cecatiello, V., De Marco, A., Blackstock, W., Kuznetsov, V., Amati, B., Mapelli, M., and Guccione, E. (2012) Symmetric dimethylation of H3R2 is a newly identified histone mark that supports euchromatin maintenance. *Nat. Struct. Mol. Biol.* **19,** 136–144
21. Buisson, R., Dion-Côté, A. M., Coulombe, Y., Launay, H., Cai, H., Stasiak, A. Z., Stasiak, A., Xia, B., and Masson, J. Y. (2010) Cooperation of breast cancer proteins PALB2 and piccolo BRCA2 in stimulating homologous recombination. *Nat. Struct. Mol. Biol.* **17,** 1247–1254
22. Osborne, T. C., Obianyo, O., Zhang, X., Cheng, X., and Thompson, P. R. (2007) Protein arginine methyltransferase 1: positively charged residues in substrate peptides distal to the site of methylation are important for substrate binding and catalysis. *Biochemistry* **46,** 13370–13381
23. Obianyo, O., Osborne, T. C., and Thompson, P. R. (2008) Kinetic mechanism of protein arginine methyltransferase 1. *Biochemistry* **47,** 10420–10427
24. Butler, J. S., Zurita-Lopez, C. I., Clarke, S. G., Bedford, M. T., and Dent, S. Y. (2011) Protein-arginine methyltransferase 1 (PRMT1) methylates Ash2L, a shared component of mammalian histone H3K4 methyltransferase complexes. *J. Biol. Chem.* **286,** 12234–12244
25. Feng, Y., Xie, N., Jin, M., Stahley, M. R., Stivers, J. T., and Zheng, Y. G. (2011) A transient kinetic analysis of PRMT1 catalysis. *Biochemistry* **50,** 7033–7044
26. Feng, Y., Wang, J., Asher, S., Hoang, L., Guardiani, C., Ivanov, I., and Zheng, Y. G. (2011) Histone H4 acetylation differentially modulates arginine methylation by an in *cis* mechanism. *J. Biol. Chem.* **286,** 20323–20334
27. Antonysamy, S., Bonday, Z., Campbell, R. M., Doyle, B., Druzina, Z., Gheyi, T., Han, B., Jungheim, L. N., Qian, Y., Rauch, C., Russell, M., Sauder, J. M., Wasserman, S. R., Weichert, K., Willard, F. S., Zhang, A., and Emtage, S. (2012) Crystal structure of the human PRMT5:MEP50 complex. *Proc. Natl. Acad. Sci. U.S.A.* **109,** 17960–17965
28. Strahl, B. D., Briggs, S. D., Brame, C. J., Caldwell, J. A., Koh, S. S., Ma, H., Cook, R. G., Shabanowitz, J., Hunt, D. F., Stallcup, M. R., and Allis, C. D. (2001) Methylation of histone H4 at arginine 3 occurs *in vivo* and is mediated by the nuclear receptor coactivator PRMT1. *Curr. Biol.* **11,** 996–1000
29. Pal, S., Baiocchi, R. A., Byrd, J. C., Grever, M. R., Jacob, S. T., and Sif, S. (2007) Low levels of miR-92b/96 induce PRMT5 translation and H3R8/H4R3 methylation in mantle cell lymphoma. *EMBO J.* **26,** 3558–3569
30. Thangaraj, B., Ryan, C. M., Souda, P., Krause, K., Faull, K. F., Weber, A. P., Fromme, P., and Whitelegge, J. P. (2010) Data-directed top-down Fourier-transform mass spectrometry of a large integral membrane protein complex: photosystem II from *Galdieria sulphuraria*. *Proteomics* **10,** 3644–3656
31. Rust, H. L., Zurita-Lopez, C. I., Clarke, S., and Thompson, P. R. (2011) Mechanistic studies on transcriptional coactivator protein arginine methyltransferase 1. *Biochemistry* **50,** 3332–3345
32. Lakowski, T. M., and Frankel, A. (2009) Kinetic analysis of human protein arginine *N*-methyltransferase 2: formation of monomethyl- and asymmetric dimethyl-arginine residues on histone H4. *Biochem. J.* **421,** 253–261

33. Siarheyeva, A., Senisterra, G., Allali-Hassani, A., Dong, A., Dobrovetsky, E., Wasney, G. A., Chau, I., Marcellus, R., Hajian, T., Liu, F., Korboukh, I., Smil, D., Bolshan, Y., Min, J., Wu, H., Zeng, H., Loppnau, P., Poda, G., Griffin, C., Aman, A., Brown, P. J., Jin, J., Al-Awar, R., Arrowsmith, C. H., Schapira, M., and Vedadi, M. (2012) An allosteric inhibitor of protein arginine methyltransferase 3. *Structure* **20,** 1425–1435
34. Schurter, B. T., Koh, S. S., Chen, D., Bunick, G. J., Harp, J. M., Hanson, B. L., Henschen-Edman, A., Mackay, D. R., Stallcup, M. R., and Aswad, D. W. (2001) Methylation of histone H3 by coactivator-associated arginine methyltransferase 1. *Biochemistry* **40,** 5747–5756
35. Obianyo, O., and Thompson, P. R. (2012) Kinetic mechanism of protein arginine methyltransferase 6 (PRMT6). *J. Biol. Chem.* **287,** 6062–6071
36. Dillon, M. B., Rust, H. L., Thompson, P. R., and Mowen, K. A. (2013) Automethylation of protein arginine methyltransferase 8 (PRMT8) regulates activity by impeding *S*-adenosylmethionine sensitivity. *J. Biol. Chem.* **288,** 27872–27880
37. Sayegh, J., Webb, K., Cheng, D., Bedford, M. T., and Clarke, S. G. (2007) Regulation of protein arginine methyltransferase 8 (PRMT8) activity by its N-terminal domain. *J. Biol. Chem.* **282,** 36444–36453
38. Wang, L., Charoensuksai, P., Watson, N. J., Wang, X., Zhao, Z., Coriano, C. G., Kerr, L. R., and Xu, W. (2013) CARM1 automethylation is controlled at the level of alternative splicing. *Nucleic Acids Res.* **41,** 6870–6880
39. Boffa, L. C., Karn, J., Vidali, G., and Allfrey, V. G. (1977) Distribution of N^G, N^G,N^G-dimethylarginine in nuclear protein fractions. *Biochem. Biophys. Res. Commun.* **74,** 969–976
40. Thandapani, P., O'Connor, T. R., Bailey, T. L., and Richard, S. (2013) Defining the RGG/RG motif. *Mol. Cell* **50,** 613–623
41. Cheng, D., Côté, J., Shaaban, S., and Bedford, M. T. (2007) The arginine methyltransferase CARM1 regulates the coupling of transcription and mRNA processing. *Mol. Cell* **25,** 71–83
42. Branscombe, T. L., Frankel, A., Lee, J. H., Cook, J. R., Yang, Z., Pestka, S., and Clarke, S. (2001) PRMT5 (Janus kinase-binding protein 1) catalyzes the formation of symmetric dimethylarginine residues in proteins. *J. Biol. Chem.* **276,** 32971–32976
43. Beck, H. C., Nielsen, E. C., Matthiesen, R., Jensen, L. H., Sehested, M., Finn, P., Grauslund, M., Hansen, A. M., and Jensen, O. N. (2006) Quantitative proteomic analysis of post-translational modifications of human histones. *Mol. Cell. Proteomics* **5,** 1314–1325
44. Golebiowski, F., and Kasprzak, K. S. (2005) Inhibition of core histones acetylation by carcinogenic nickel(II). *Mol. Cell. Biochem.* **279,** 133–139
45. Cheung, W. L., Ajiro, K., Samejima, K., Kloc, M., Cheung, P., Mizzen, C. A., Beeser, A., Etkin, L. D., Chernoff, J., Earnshaw, W. C., and Allis, C. D. (2003) Apoptotic phosphorylation of histone H2B is mediated by mammalian sterile twenty kinase. *Cell* **113,** 507–517
46. Zoroddu, M. A., Kowalik-Jankowska, T., Kozlowski, H., Molinari, H., Salnikow, K., Broday, L., and Costa, M. (2000) Interaction of Ni(II) and Cu(II) with a metal binding sequence of histone H4: AKRHRK, a model of the H4 tail. *Biochim. Biophys. Acta* **1475,** 163–168
47. Allahverdi, A., Yang, R., Korolev, N., Fan, Y., Davey, C. A., Liu, C. F., and Nordenskiöld, L. (2011) The effects of histone H4 tail acetylations on cation-induced chromatin folding and self-association. *Nucleic Acids Res.* **39,** 1680–1691
48. Luger, K., Mäder, A. W., Richmond, R. K., Sargent, D. F., and Richmond, T. J. (1997) Crystal structure of the nucleosome core particle at 2.8 Å resolution. *Nature* **389,** 251–260
49. Chodaparambil, J. V., Barbera, A. J., Lu, X., Kaye, K. M., Hansen, J. C., and Luger, K. (2007) A charged and contoured surface on the nucleosome regulates chromatin compaction. *Nat. Struct. Mol. Biol.* **14,** 1105–1107
50. Zhou, J., Fan, J. Y., Rangasamy, D., and Tremethick, D. J. (2007) The nucleosome surface regulates chromatin compaction and couples it with transcriptional repression. *Nat. Struct. Mol. Biol.* **14,** 1070–1076
51. Fingerman, I. M., Li, H. C., and Briggs, S. D. (2007) A charge-based interaction between histone H4 and Dot1 is required for H3K79 methylation and telomere silencing: identification of a new trans-histone pathway. *Genes Dev.* **21,** 2018–2029
52. Parra, M. A., Kerr, D., Fahy, D., Pouchnik, D. J., and Wyrick, J. J. (2006) Deciphering the roles of the histone H2B N-terminal domain in genome-wide transcription. *Mol. Cell. Biol.* **26,** 3842–3852
53. Wyrick, J. J., and Parra, M. A. (2009) The role of histone H2A and H2B post-translational modifications in transcription: a genomic perspective. *Biochim. Biophys. Acta* **1789,** 37–44
54. Casadio, F., Lu, X., Pollock, S. B., LeRoy, G., Garcia, B. A., Muir, T. W., Roeder, R. G., and Allis, C. D. (2013) H3R42me2a is a histone modification with positive transcriptional effects. *Proc. Natl. Acad. Sci. U.S.A.* **110,** 14894–14899
55. Li, Q., Zhou, H., Wurtele, H., Davies, B., Horazdovsky, B., Verreault, A., and Zhang, Z. (2008) Acetylation of histone H3 lysine 56 regulates replication-coupled nucleosome assembly. *Cell* **134,** 244–255
56. Cho, E. C., Zheng, S., Munro, S., Liu, G., Carr, S. M., Moehlenbrink, J., Lu, Y. C., Stimson, L., Khan, O., Konietzny, R., McGouran, J., Coutts, A. S., Kessler, B., Kerr, D. J., and Thangue, N. B. (2012) Arginine methylation controls growth regulation by E2F-1. *EMBO J.* **31,** 1785–1797